NATIONAL ENERGY TECHNOLOGY LABORATORY

Results from an Aeromagnetic Survey to Detect Steel-Cased Wells at a Marcellus Shale Well Site in Washington County, Pennsylvania

5 November 2024

U.S. Department of ENERGY | NATIONAL ENERGY TECHNOLOGY LABORATORY

Office of Fossil Energy and Carbon Management

DOE/NETL-2025/4891

Disclaimer

Cover Illustration: A CGG Midas II helicopter magnetic surveying system with two boom-mounted cesium magnetometers was used to locate legacy wells by detecting the distinctive magnetic signature of vertical steel well casing.

Suggested Citation: Veloski, G. A.; Hammack, R. W.; Sams, III, J. E. *Results from an Aeromagnetic Survey to Detect Steel-Cased Wells at a Marcellus Shale Well Site in Washington County, Pennsylvania*; DOE.NETL-2025.4891; NETL Technical Report Series; U.S. Department of Energy, National Energy Technology Laboratory: Pittsburgh, PA, 2024; p 112. https://doi.org/10.2172/2477972.

An electronic version of this report can be found at:

https://netl.doe.gov/energy-analysis/search

Results from an Aeromagnetic Survey to Detect Steel-Cased Wells at a Marcellus Shale Well Site in Washington County, Pennsylvania

Garret A. Veloski[1]; Richard W. Hammack[1]; James E. Sams, III[1]

[1] National Energy Technology Laboratory, 626 Cochran Mill Road, Pittsburgh, PA 15236, USA

DOE/NETL-2025/4891

5 November 2024

NETL Contacts:

Rick Hammack, Principal Investigator

Natalie Pekney, Technical Portfolio Lead

Bryan Morreale, Associate Laboratory Director for Research & Innovation, Research & Innovation Center

This page intentionally left blank.

Table of Contents

This page intentionally left blank.

List of Figures

List of Tables

This page intentionally left blank.

Acronyms, Abbreviations, and Symbols

Term	Description
AGL	Above ground level
BTEX	Benzene, Toluene, Ethyl benzene, and Xylene
CRADA	Cooperative Research and Development Agreement
DC	Direct current
DIAL	DIfferential Absorption LiDAR
DOE	U.S. Department of Energy
DOQQ	Digital Ortho Quarter Quadrangle
EOR	Enhanced oil recovery
ER	Earth resistivity
FAA	Federal Aviation Administration
GIS	Geographical Information System
GPS	Global Positioning System
LiDAR	Light Detection and Ranging
NETL	National Energy Technology Laboratory
NORM	Naturally Occurring Radioactive Materials
NPR	Naval Petroleum Reserve
PADEP	Pennsylvania Department of Environmental Protection
PA/IRIS/WIS	Pennsylvania's Internet Record Imaging System/Wells Information System
TD	Total depth
TF	Total field
TMI	Total magnetic intensity

Acknowledgments

The aeromagnetic survey described in this report was completed as part of the National Energy Technology Laboratory's (NETL) research for the U.S. Department of Energy's (DOE) Complementary Research Program under Section 999 of the Energy Policy Act of 2005. A subsequent ground investigation and analysis was performed under provisions of the Bipartisan Infrastructure Law, which contained language requesting that DOE collaborate with the Interstate Oil and Gas Compact Commission (IOGCC) and develop a program focused around reducing the impact of undocumented orphaned wells (UOWs). This report addresses well location, the first step in the remediation of UOWs.

The authors wish to acknowledge landowners who allowed access to their property for ground verification of well targets from the aeromagnetic survey.

EXECUTIVE SUMMARY

Pennsylvania has a 150-year history of oil and gas production—the longest of any state—and this enduring activity has resulted in the drilling of more than 300,000 recorded wells. However, unknown wells likely exist because innumerable wells were drilled during Pennsylvania's intense early oil and gas history when incomplete records were kept of well locations. There is concern that early wells are likely to be ineffectively sealed because there were no laws that required plugging when the wells were abandoned. Today, many undocumented and unplugged wells are thought to be in areas of emerging shale gas and shale oil development where open wellbores can provide a pathway for undesired upward migration of fluids and gas from hydraulically fractured reservoirs. Due to this concern, Pennsylvania regulators have asked operators to locate orphaned and abandoned wells within a 1,000-ft buffer of proposed new wells. The objective of this report is to demonstrate that high-resolution aeromagnetic surveys, historic air photos, and Light Detection and Ranging (LiDAR) imagery can be rapid and effective methods to reconnoiter large, forested areas of moderate terrain for the presence of abandoned wells. These well-finding methods were evaluated at a proposed Marcellus Shale gas drilling site in Washington County, Pennsylvania, where the methods collectively located 18 confirmed wells: 15 wells were identified from aeromagnetic surveys, two wells were identified from inspection of historical air photos, and one well was identified by evaluation of state-wide LiDAR imagery. Only six wells were previously known, and their locations, as recorded in Pennsylvania's statewide oil and gas wells database (PA/IRIS/WIS), were often too inaccurate for the wells to be found in the dense underbrush. Twelve wells identified in this study were abandoned, unmarked, and undocumented.

Aeromagnetic surveys locate wells by detecting the unique magnetic signature of vertical, steel well casing, which is depicted on magnetic maps as a "bull's eye" type anomaly that is centered directly over the well. However, when wells were drilled and found to be sub-economic, their casing was sometimes pulled and salvaged for reuse. Such wellbores provide no magnetic response and go undetected if all casing was removed. Oftentimes attempts to retrieve well casing were not 100% successful. For example, historical records for one well in the study area indicate that the well was completed in 1902 as a dry hole and that, to the extent possible, the casing was pulled for reuse. However, a section of 10-in. diameter steel casing was not recovered and remains at an unknown depth in the wellbore. This well was easily detected by the aeromagnetic survey although only deep casing remained in the well.

To mitigate for the likelihood that wellbores exist where most or all casing has been removed, this study augmented aeromagnetic data with historic air photos and digital terrain models generated from LiDAR datasets—both databases are publicly available at no cost for areas within Pennsylvania. These complementary methods located three wells where the aeromagnetic anomaly, although present, was subtle and overlooked. Together, these methods determined accurate locations for six known wells within the study area and located 12 previously unknown wells. Although it is not certain that these methods successfully located all wells in the study area, the application of these methods does represent a significant improvement over relying on existing databases for well locations.

1. INTRODUCTION

Unplugged, abandoned oil and gas wells allow fluid and gas from subsurface formations to migrate unimpeded to the surface which can result in fire and explosion hazards (e.g., volatile hydrocarbons), human health impacts from inhalation (radon, hydrogen sulfide, and carbon dioxide), and contamination of underground drinking water sources (brine; Benzene, Toluene, Ethyl benzene, and Xylene (BTEX)), and naturally occurring radioactive materials (NORM). Where legacy oil and gas fields coincide with residential, commercial, and industrial areas, efforts should be made to locate, evaluate, and plug (if necessary) existing wells. Often, the challenge is locating wells because many wells may have been drilled and abandoned before accurate records were kept of their locations. Surface indicators of a well's location (e.g., derricks, wellheads, tanks, and flow lines) may have been removed and markers denoting the location of abandoned wells are easily overlooked in areas of heavy vegetation.

Wellbores penetrating coal seams were found hazardous to mining in the Appalachian region especially after the advent of the longwall technique (Armstrong, 1973). Methods that employed handheld metal detectors and portable hydrocarbon analyzers were developed to help the mining industry locate existing wellbores. Well location efforts generally start with an investigation of recorded information such as well plats, county and company development maps, as well as state agency well maps and databases. Some of these resources are better organized than others, especially those that incorporate well logging records, owner information, production history, casing schedules, status, and interactive mapping and querying capabilities. One good example of well information example resources is the state of Wyoming's Oil & Gas Conservation Commission's online database (WOGCC Data Explorer (wyo.gov)).

Historically, improperly abandoned wellbores have played a key role in dangerous explosions resulting from the migration of stray gas into buildings, sometimes with fatalities. Examples of this have been documented in case histories (Baer et al., 1995; Xia and Williams, 2003). Xia et al. (2003) used ground-based magnetic surveys to successfully locate steel-cased brine wells in Hutchinson, Kansas, after unplugged wells had allowed natural gas to rise to the surface and ignite, causing fatalities and structural damage. Versailles Borough, Pennsylvania, has also recorded incidents ranging from illness to home explosions believed to be caused by stray gas from numerous, closely spaced, unmarked, and unsealed natural gas wells. The U.S. Department of Energy's (DOE) National Energy Technology Laboratory (NETL) used magnetic and methane surveys to locate more than 50 targets within Versailles Borough that were likely wells (two targets were excavated and confirmed to be gas wells) (Hammack and Veloski, 2015). In 2005, Anadarko Petroleum Corporation asked NETL to locate abandoned oil and natural gas wells in the Salt Creek Oilfield near the town of Midwest, Wyoming, where unmarked and abandoned, unplugged wells lie buried a few meters belowground within a populated area. It was essential that these wells be located and either plugged or re-worked prior to conducting enhanced oil recovery (EOR) using supercritical CO_2—flooding and water—flooding operations. Many wells were found to be near occupied dwellings where they posed not only an explosion risk (from natural gas ignition), but also a toxicity risk from hydrogen sulfide, and an asphyxiation risk from CO_2. NETL employed a portable global positioning system (GPS)-linked, cesium-ion vapor magnetometer (Figure 1) and geographical information system (GIS) mapping resources to successfully locate 23 wells whose locations were not accurately known previously; each well location was verified by excavation to expose the top of casing. Historical records

from the local library and museum and a geo-referenced historical air photo were used to assign well IDs to each uncovered well.

Advances in magnetometer design have reduced orientation errors, increased sensitivity, and now offer GPS-linked data at high sampling rates by incorporating tablet-PC data acquisition systems. Differentially corrected GPS navigation systems brought further improvements in survey planning that result in more uniform coverage and better reproducibility. These systems also allow easy correction of diurnal effects, data lag, and other post-processing operations used for mapping and modeling magnetic anomalies (Breiner, 1973). Nonetheless, ground magnetic surveys over large areas for steel-casing wells are tedious and time consuming. Ubiquitous buried ferrous metal trash can also complicate the interpretation of magnetic anomalies. However, collecting magnetic data over a relatively large area (>1 square kilometer (km^2) from an airborne platform vastly outperforms all other modalities. In 1985, Freischknecht et al. (1985) successfully used a turbine-powered, fixed-wing aircraft to perform magnetic surveys for locating wellheads in Oklahoma. This system used a proton precession magnetometer and was one of the first to use flight path recovery (before GPS), accurate barometric and radar altimetry, and applied compensation for so-called maneuver noise. This survey also employed one or more magnetic-base stations for post-processing correction of diurnal magnetic effects.

In 2005, NETL and Anadarko Petroleum Corporation (through a Cooperative Research and Development Agreement or CRADA) evaluated a unique helicopter magnetometer system (Fugro Midas II) for its ability to accurately locate thousands of known wells and many unmarked and abandoned wells within the Salt Creek Oilfield in east-central Wyoming (Hammack et al., 2006). NETL was provided a 1 square mile (mi^2) test area within the oilfield where an intense ground search was conducted to locate all existing wells. The locations of well-type magnetic anomalies identified by the helicopter survey were then compared with confirmed well locations from the ground survey. The helicopter magnetic survey detected 131 of the 141 wells located by the ground survey, but more importantly, the helicopter survey successfully located 100% of the wells drilled for primary production (pre-1926), the wells that are most often unrecorded and unmarked. The helicopter magnetic survey at Salt Creek Oilfield showed that survey line orientation (relative to magnetic north), terrain compliance, and interline spacing interval were key factors to consider in survey design.

Other potential airborne well-finding technologies were evaluated during this study, including methane detection using Light Detection and Ranging (LiDAR), DIfferential Absorption LiDAR (DIAL), and Naturally Occurring Radioactive Material (NORM) detection using airborne radiometry. The DIAL survey detected methane emissions from active oilfield operations, including wells with operating pump jacks but did not identify the locations of any previously unknown, abandoned wells. The airborne radiometric survey was intended to identify abandoned well locations by detecting anomalous gamma emissions from NORM-bearing scale deposits in flow pipes and tank bottoms that may have been left on location when wells were abandoned. However, the gamma anomalies located by the helicopter survey correlated to the outcrop of certain shale units (high gamma) and the location of a highway where igneous rock was used as fill (low gamma); no well sites were located based on gamma irradiation from NORM.

In 2007, NETL engaged in an intra-agency project to map 1,353 recorded wells and an unknown number of unrecorded wells at the Naval Petroleum Reserve No. 3 (NPR No. 3) (Veloski et al., 2008), a U.S. DOE facility in the Teapot Dome Oilfield (Friedman and Stamp, 2005) just a few miles south of the Salt Creek Oilfield project site. The helicopter magnetic survey at NPR No. 3

used the same system (Fugro Midas II) as the previous survey at Salt Creek Oilfield although the NPR No. 3 survey was flown at a lower altitude (nominal 20-m above ground level (AGL) and with a closer spacing (25 m) between parallel survey lines. Because the magnetic response from some post-1960 wells in the Salt Creek Oilfield survey was too weak to be detected by a helicopter magnetic survey when flown at 35-m altitude, the NPR No. 3 survey was flown at a lower altitude (where possible) to detect wells with weaker magnetic anomalies. Closer line spacing was used to improve spatial resolution because the well density was high in some areas of NPR No. 3 and magnetic anomalies from closely spaced wells were expected to overlap. The helicopter magnetic survey at NPR No. 3 located 2,355 magnetic anomalies, which included both well and non-well targets. The well inventory for NPR No. 3 contained 1,353 well locations; only 889 of 1,353 well records (66%) matched airborne or ground magnetic targets to within 15 m, an indicator of spatial inaccuracies inherent in historic well location databases. The remaining 1,466 magnetic anomalies could not be correlated with well locations in the NPR No. 3 well inventory and are likely to be undocumented wells, documented wells with inaccurate locations, or ferro-metallic oilfield infrastructures.

Ground verification of well targets from the helicopter magnetic survey at NPR No. 3 was conducted on a 0.5 km^2 test area that contained 75 closely spaced wells according to the well database. The helicopter magnetic survey identified 28 well targets within the test area which were co-located with well locations confirmed by the ground survey. The ground survey located 29 wells, one more than targeted by the helicopter magnetic survey. Forty-six wells in the NPR No. 3 database for the test area could not be located on the ground and were not targeted by helicopter magnetic data. Of the 46 unfound and untargeted wells, 42 were less than 162 m in total depth and were designated as plugged and abandoned. Because no well-type magnetic anomalies were detected at these 42 well locations during the airborne and ground magnetic surveys, it can be assumed that most, if not all casing was removed from these wells when abandoned.

The current study was undertaken to determine if the helicopter magnetic surveys that successfully located wells in Wyoming oilfields could also be applied to legacy wells in western Pennsylvania where wells are older, the terrain is more rugged, and dense vegetation obscures surface evidence of abandoned well locations. The motivation for this research is that there are estimated to be between 305,000 and 390,000 wells in northern and western Pennsylvania drilled over the Commonwealth's 150-year history of oil and gas development (Dilmore et al., 2015). Because Pennsylvania only began permitting wells in 1957 (Commonwealth of Pennsylvania, 2024), the number and location of wells drilled before that time is incomplete. Moreover, early wells may not be effectively sealed because there were no laws at that time that mandated plugging when wells were abandoned. Now, many unrecorded and possibly unplugged wells are thought to be in areas of unconventional oil and gas development where their wellbores may provide a pathway for undesired upward migration of fluids and gas from hydraulically fractured reservoirs. The risk will undoubtedly increase with the expansion of unconventional gas and oil well drilling into Upper Devonian/Lower Mississippian shale and sandstone formations that are closer to the penetration depths of the old wells. Because of this concern, Pennsylvania regulators have asked operators to locate orphaned and abandoned wells within a 1,000-ft-buffer of proposed new wells.

1.1 SITE DESRIPTION

The ability of helicopter magnetic surveys to locate abandoned wells was tested at a 3.1 km^2 study area in Washington County, Pennsylvania (Figure 2), that contains a well pad with five horizontal Marcellus Shale gas wells completed in 2014 and an unknown number of older vertical wells. Washington County has had a long history of continuous oil and gas production dating from the late 1800s (Figure 3), and there are six abandoned or producing vertical wells within the study area based on records obtained from the Pennsylvania Department of Environmental Resources (PA Oil and Gas Mapping, 2024). The area also contains gas transmission pipelines, power lines, primary dwellings, private water wells, outbuildings, barns, and other cultural sources that may give rise to magnetic anomalies.

The study area lies within the Pittsburgh Low Plateau Section of the Appalachian Plateau Physiographic Province, which is described as "a smooth to irregular, undulating surface cut by numerous, narrow, relatively shallow valleys" (Sevon, 2000). Topography within the study area is of moderate relief with rounded hills separated by valleys containing first order streams. The drainage pattern is dendritic.

Surface geology of the study area consists of Upper Pennsylvanian age shale, siltstone, sandstone, limestone, and coal of the Washington Formation and the underlying Monongahela Group. The study area is on the southwestern limb of the northwest trending Cross Creek Syncline. Strata within the study area dip gently toward the northeast. The Pittsburgh Coalbed, which occurs at the base of the Monongahela Group, has been mined from underground workings in the northwestern portion of the study area.

The study area is primarily hardwood forest with subordinate areas of shrubland and grassland (overgrown fields) that have been managed for wildlife values. The successional plants that typify the transition from farmland back to forest are often an impenetrable mass of thorny, briery vegetation that makes the ground search to locate wells difficult, unpleasant, and often unsuccessful.

The study area is classified as a continental climate and receives an average annual precipitation of 938 mm with the wettest months occurring in May, June, and July (http://www.pittsburgh-pit.airports-guides.com/pit_climate.html; accessed on December 9, 2021).

Figure 1: Ground-based survey employing a GPS-linked cesium-ion magnetometer.

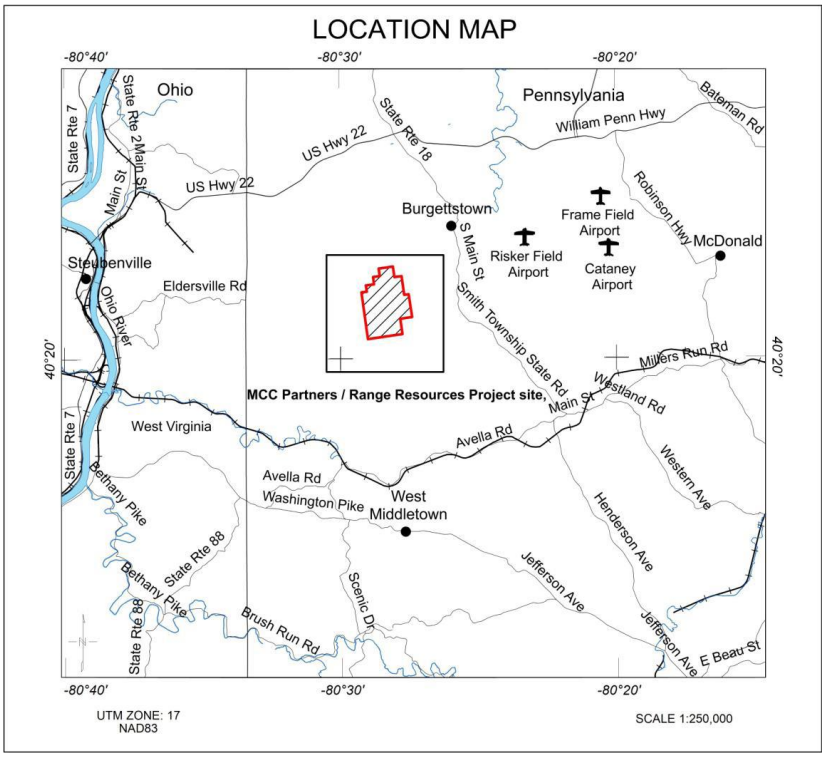

Figure 2: Location map for the Washington County Site, Pennsylvania, airborne magnetic survey.

1.2 AEROMAGNETIC SURVEY DESIGN

A turbine-powered helicopter was used that had two boom-mounted magnetic sensors spaced 12.9 m apart and oriented orthogonal to the flightpath. A helicopter-mounted system provides the performance of short take-off and landing operations, the utility of slow flight, terrain compliance, and the economy of short turn-around distance. Appliances may also be installed on the exterior of the aircraft without appreciably altering flight characteristics. The survey design used to fly the Washington County site consisted of simple parallel swaths oriented in a north-south direction. A north-south traverse line orientation will show the maximum peak to peak amplitude for a given magnetic anomaly (Breiner, 1973). At the survey location, the local magnetic variation (declination) was 8.9° west. Therefore, the optimum nominal survey flight line direction would be oriented 360° – 8.9°= 351.1° (geographical). The helicopter magnetic survey was flown in a serpentine pattern with bidirectional flight line azimuths of 352° and 172°.

The survey design was optimized based on experience from previous magnetic surveys. The main flight plan comprised parallel flight lines totaling 263.1-line km that were flown at 25-m spacing and 352° or 172° azimuth. Tie lines (26.4-line km at 250 m spacing) for leveling magnetic data were oriented orthogonal to the survey course (82° or 262° azimuth). There was a minimum line length criterion of 1 km. The majority of the 660-hectare survey area was sparsely populated, and the airspace is designated class G, which simplified adherence to Federal Aviation Administration (FAA) operating regulations at the survey altitude. Other considerations in the design included terrain/obstruction conflicts, power lines, residential areas, and busy roads. Fugro Airborne Surveys further restricted their flights to avoid occupied dwellings.

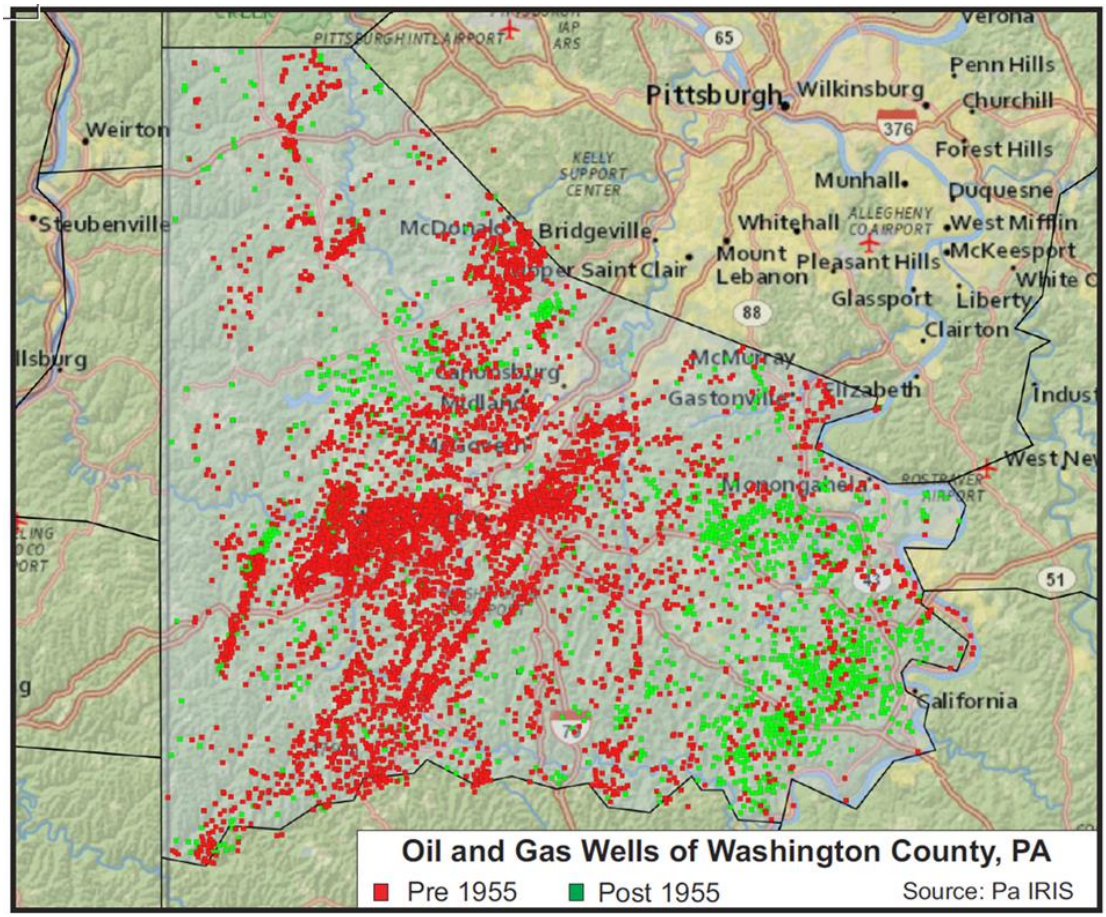

Figure 3: Distribution of recorded oil and gas wells in Washington County, Pennsylvania. Prior to 1957, there was no well registration requirement (58 Pa. Stat. Ann. §601.203).

1.3 MAGNETIC ANOMALIES

The total magnetic intensity (TMI) measured by the magnetometer is a scalar value derived from the Earth's total magnetic field vector independent of direction. A magnetometer is used to measure spatial variations of the Earth's total magnetic field. Anomalies are perturbations of the Earth's magnetic field caused by induced and remanent components of magnetization (Breiner, 1973). Induced magnetic anomalies are largely the result of the Earth's ambient magnetic field acting on an object, which creates a magnetic moment. The magnitudes of induced anomalies are proportional to the Earth's field and greatly influenced by the magnetic susceptibility (k) of the material (Equation 1). The intensity is related to the size, shape, and orientation of the source, and its distance from the sensor (Barrows and Rocchio, 1990). In general, large ferrous metal objects give rise to large anomalies; and a small, highly magnetized object produces a strong anomaly from a short distance. The intensity of magnetic anomalies varies with distance according to orientation in the Earth's magnetic field as shown in Equations 2-4. For the survey latitude (approx. 40° north), the Earth's magnetic field is steeply inclined, roughly parallel (local magnetic inclination 67.8°), and thus the observed anomalies from the typical vertically oriented steel well casing will approximate the appearance of a bull's-eye (monopole) when the magnetic signal intensity is contoured over several traverse lines (Barret, 1931; Martinek, 1988). The true

location of the feature relative to the traverse is likely to lie off to one side of a given line. On the ground, the approximate well location can be determined by finding the peak intensity along a line and constructing a traverse perpendicular to that location. Anomalies become more subdued and tend to broaden with depth (distance) from the source. Magnetic anomalies appearing in an aerial survey are likely to be superimposed on a low frequency regional magnetic gradient or trend that may be removed from the dataset during further processing.

Remanent or permanent magnetization is mainly a characteristic of ferrous metal objects. The magnitude of permanent magnetism can be substantial, and largely dependent on metallurgical properties of the steel which affects the magnetic susceptibility (k). Mechanical impact and direct current (DC) welding are also factors that may impart permanent magnetization. The magnetometer measures the net resultant magnetic field intensity which is the sum of induced and remanent fields ($I_{obs}= I_{induced +} I_{remanent}$). Permanent magnetization in a ferromagnetic object may oppose the induced component and appear as a net negative anomalous feature. Because the intensity and direction of permanent magnetization is generally unknown, the observed anomalous magnetization is assumed to be based upon induced magnetization alone. A relatively high degree of permanent magnetization was noted in cable tool drilled wells (Bowman, 1911). This was attributed to mechanical action, heating, and contact with large electromagnets sometimes used as fishing tools. NETL confirmed this observation in pre-1930 cable tool wells at NPR No. 3. These wells exhibited a much higher TMI when compared to wells drilled after ~1970 (Veloski et al., 2008).

Induced magnetization and magnetic moment:

$$\text{Induced Magnetization } I=kF \tag{1}$$

where k= magnetic susceptibility, which for iron and steel is typically between 1–10 cgs units and F= Earth's ambient field in gauss (~0.534 gauss or 53,400 nanoteslas for site).

The magnetic moment can be calculated using the expression:

$$M=kFV$$

F= Earth's ambient field in gauss (~0.534 gauss for site) and V=volume in cm^3.

TMI varies with distance and orientation in Earth's field according to the following relationships:

$$TMI=M/r^2 \text{ (monopole*, from any direction)} \tag{2}$$

*A vertically oriented pipe or well casing is a dipole, although it appears monopolar having only a minor negative component in the profile.

$$TMI=M/r^3 \text{ (dipole, along line and perpendicular)} \tag{3}$$

$$TMI =2M/r^3 \text{ (dipole, along axis and off one end)} \tag{4}$$

where r= distance between magnetized object and sensor.

2. OBSERVATIONS

2.1 RESULTS FROM THE AIRBORNE SURVEY AT THE WASHINGTON COUNTY SITE

The airborne magnetic data from the March 9-10, 2012 survey were processed according to the flowchart in Appendix B of the attached Fugro Geophysical Survey Report 12024 prepared for the U.S. DOE. A total of 289.5-line km of magnetic data was collected in 110 flight lines over 660 hectares, resulting in 148,468 data samples per sensor. The cost per line kilometer, including tie lines was $270 (2012 dollars). The elevation within the surveyed area ranges from 330 m to 442 m mean sea level. The laser altimeter on the helicopter ranged from 22.4 m to 65.2 m above ground level (average 40.4 m, standard deviation 6.3 m) during the survey. Terrain compliance was consistent throughout. The data were corrected for the magnetic influence from the aircraft's remanence (heading error) and induced magnetic effects from electrical currents aboard the helicopter, as well as effects caused by moving through the Earth's magnetic field (maneuver noise) (Luyendyk, 1997). These corrections are collectively referred to as compensation.

The deliverables from the airborne contractor (Fugro Airborne Surveys, Appendix B) included a DVD-ROM containing a data archive, grids, maps, geophysical report, and video archive along with two paper copies of the report. Printed maps consisting of a horizontal gradient-enhanced total magnetic intensity, calculated magnetic vertical gradient, and measured transverse magnetic gradient. When a target appeared on more than one adjacent flight line and was clearly related to a single feature, the most intense of these were counted as a single target. Where possible, the video archive was used to help classify a target based on the physical appearance of the ground directly below the aircraft, along the flight line and at the location of the recorded anomaly. The video archive contains timestamps and fiducials that are synchronized with the aeromagnetic data stream. In areas of heavy tree canopy, visual verification of targets from the video record was not possible. The target coordinates were converted by NETL to file formats that are compatible with GPS receivers, GIS, and web-based viewing software. Universal exchange format facilitates upload to various compliant GPS models as waypoints for field navigation to aid in the reconnaissance. These waypoints may then be converted to keyhole markup language (kml) and ArcGIS™ shapefile formats for sharing with colleagues and industry partners as layers in Google Earth™ and ESRI GIS software products.

The airborne contractor selected 144 magnetic targets from the calculated vertical magnetic gradient employing the proprietary Fugro Atlas™ software. Selected magnetic targets are presented in tabular form in Appendix B. From the 144 targets, 64 were classified as "cultural," 26 "pipeline," and 59 were "unknown." Several of the "unknown" target class were spatially related to the approximate positions of known wells. Other targets found near residences, were most likely steel-cased private water wells and were not investigated (Figure 3). The contractor did not classify any targets as suspected wells, nor were they able to visibly discern well targets from the video archive. NETL reclassified certain targets appearing on the list by comparing their location to the position information and descriptions found in the existing PAIRIS/WIS database and from geo-referenced historic air photos. Those targets reclassified as possible wells were prioritized according to location to optimize the reconnaissance effort. Landowner permission for access to the sites was obtained through a Landman having a business relationship with the lessors. Whenever an apparent well-type anomaly was investigated, but no surface evidence for a well existed, a portable magnetometer was used to locate the well casing. A

Geosoft™ line database was provided by the airborne contractor containing all the data channels acquired during the survey (Appendix B). The leveled, compensated, and diurnally corrected TMI data were gridded using minimum curvature and filtered using an analytic signal algorithm. The resulting grid was further processed into a color-draped and shaded map image to assist in the visual identification of potential well anomalies (Figure 4). Analytic signal processing effectively removes negative frequency components of the magnetic signal and enhances the edges of the features giving rise to these signals (Figures 5 and 6). Shading gives a 3D visual impression to the anomalous features. Collectively, these enhancements provide image maps that emphasize even the subtlest of magnetic anomalies. One downside is that it also tends to exaggerate certain processing flaws such as inadequate leveling that may complicate visual interpretation.

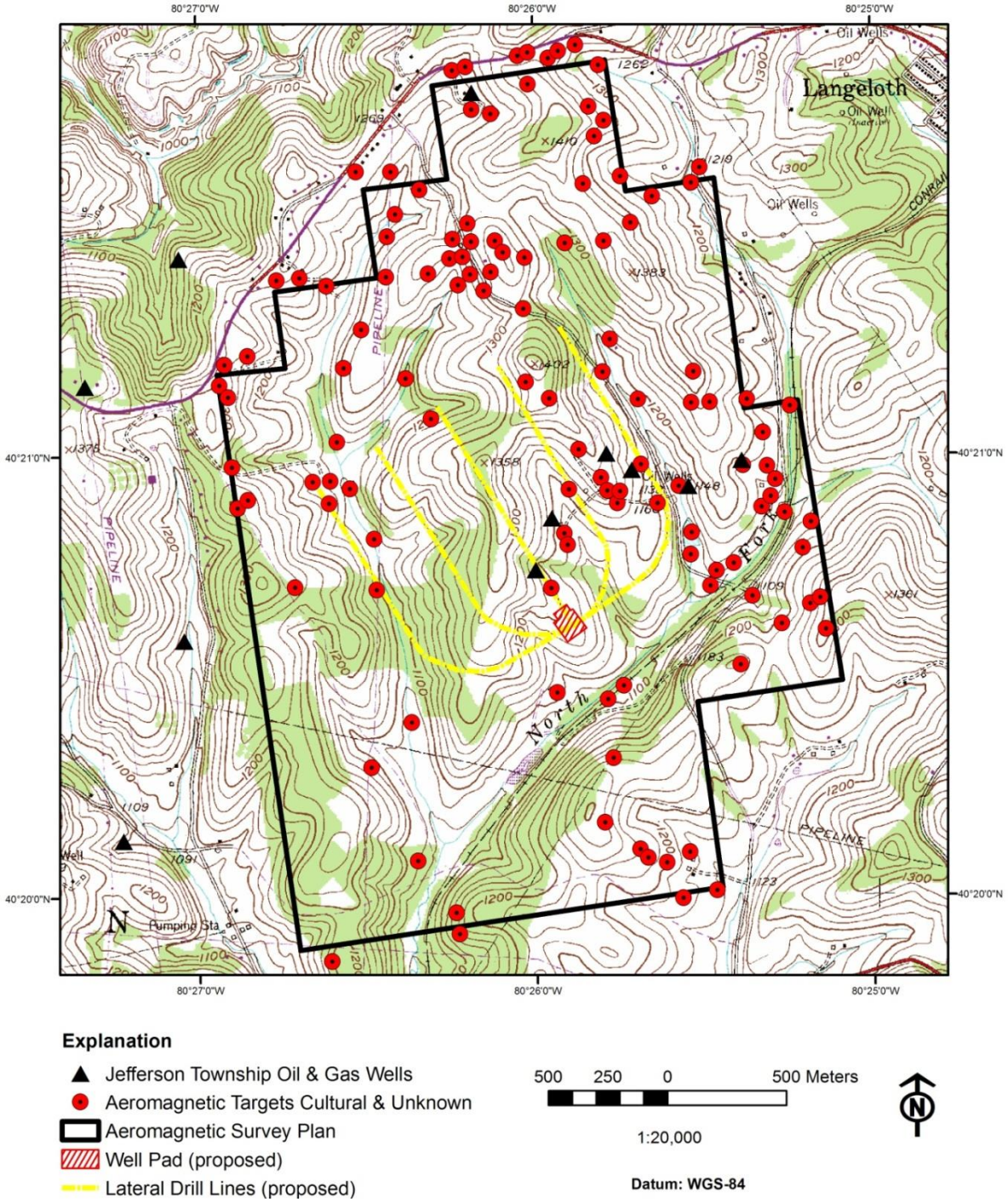

Figure 4: Map depicting locations of 123 non-pipeline related targets selected from the Midas II aeromagnetic dataset and their locations relative to known oil and gas wells at the Washington County, Pennsylvania site.

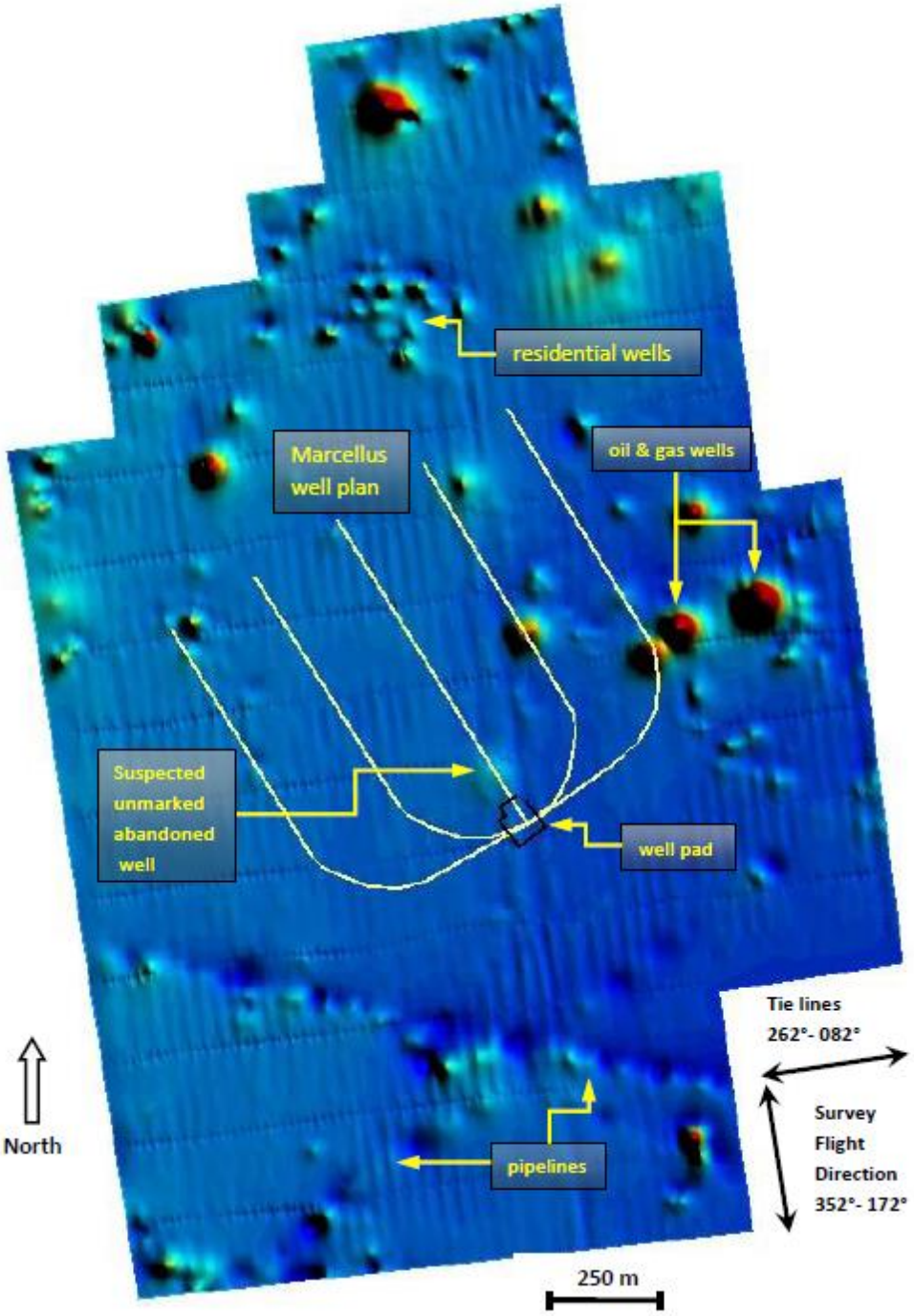

Figure 5: Enhanced Midas II aeromagnetic data acquired over the Washington County site. The flight line and tie line course artifacts are visible due to incomplete leveling in this color-draped and shaded image of the averaged TMI data for both sensors. The well pad boundary is depicted in black, the horizontal well trajectories in yellow. A broad monopole anomaly is visible just northwest of the well pad that warranted more detailed investigation.

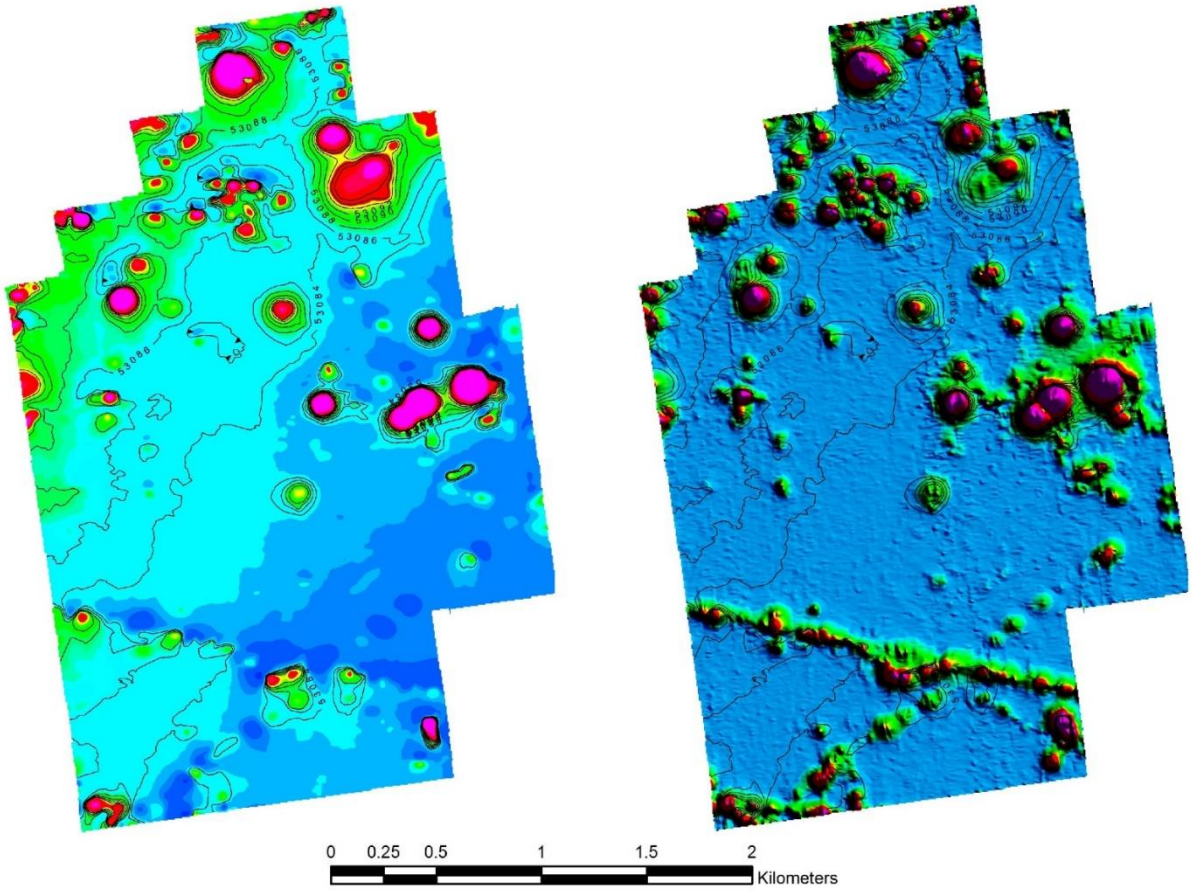

Figure 6: Images above have been compensated, diurnally corrected, and leveled TMI data from the Fugro aeromagnetic survey. The left image shows a regional magnetic gradient that increases toward the northwest. The right image was analytic signal processed and shaded to enhance positive and negative magnetic anomalies. The contour interval is 2 nT.

2.2 IDENTIFICATION OF POTENTIAL WELLS USING HISTORIC IMAGERY AND LIDAR

Anthropogenic disturbances on the ground can present as elevation anomalies in LiDAR datasets. Anomalies of this type were found to be highly effective for locating charcoal ovens used in early 1800s coke production for Pennsylvania's nascent steel industry (Sams, 2012). Figure 7 shows an overlay of aeromagnetic contours on a shaded LiDAR elevation grid. A linear anomaly in the LiDAR corresponded to a subtle depression that may be the remnants of an early road cut leading to a well site. Seven similar LiDAR features within the study area were found to coincide with aeromagnetic monopole anomalies and were subsequently confirmed to be well sites by ground reconnaissance. LiDAR was used as supporting evidence for determining potential well locations where there was uncertainty in the interpretation of the magnetic anomaly.

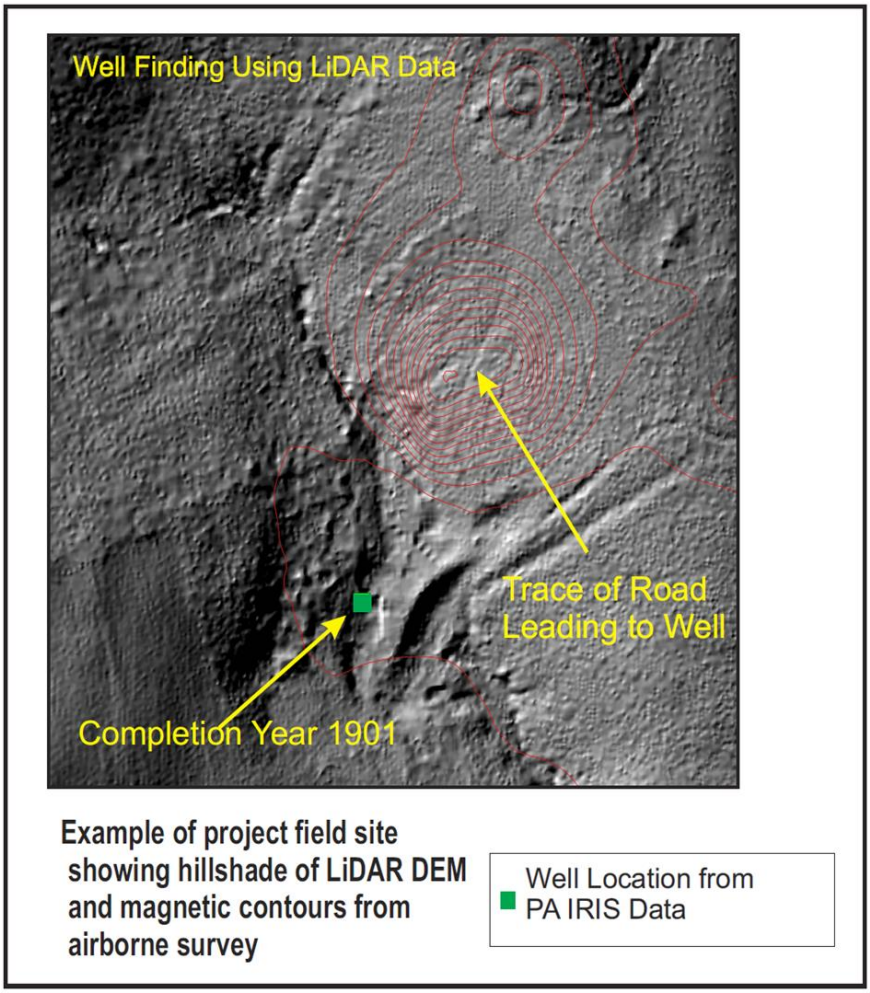

Figure 7: LiDAR anomalies can provide subtle evidence of surface disturbances that may be related to historical well development activities. Note there is an error in the PA IRIS well location, the actual well location is shown by the magnetic contours and LiDAR imagery.

Unlike LiDAR, historic aerial photographs provide unequivocal evidence for the presence of a legacy well. The 1930s imagery in Figure 8 shows three well derricks and wheelhouses, only one of which was inside the detailed ground investigation area. This non-orthographic imagery is available from the Pennsylvania Spatial Access Data Access website (Pennsylvania Spatial Data Access (psu.edu)) for most of Pennsylvania. The air photos are not geo-referenced and therefore require the manual use of ground control points to assign map coordinates. The accuracy of any geo-locations extracted from the resulting maps is highly dependent on correctly identifying features in the original imagery that can be found on modern aerial reference imagery (Digital Ortho Quarter Quadrangles, DOQQs). Six well sites in the study area could be seen in the geo-referenced historic images.

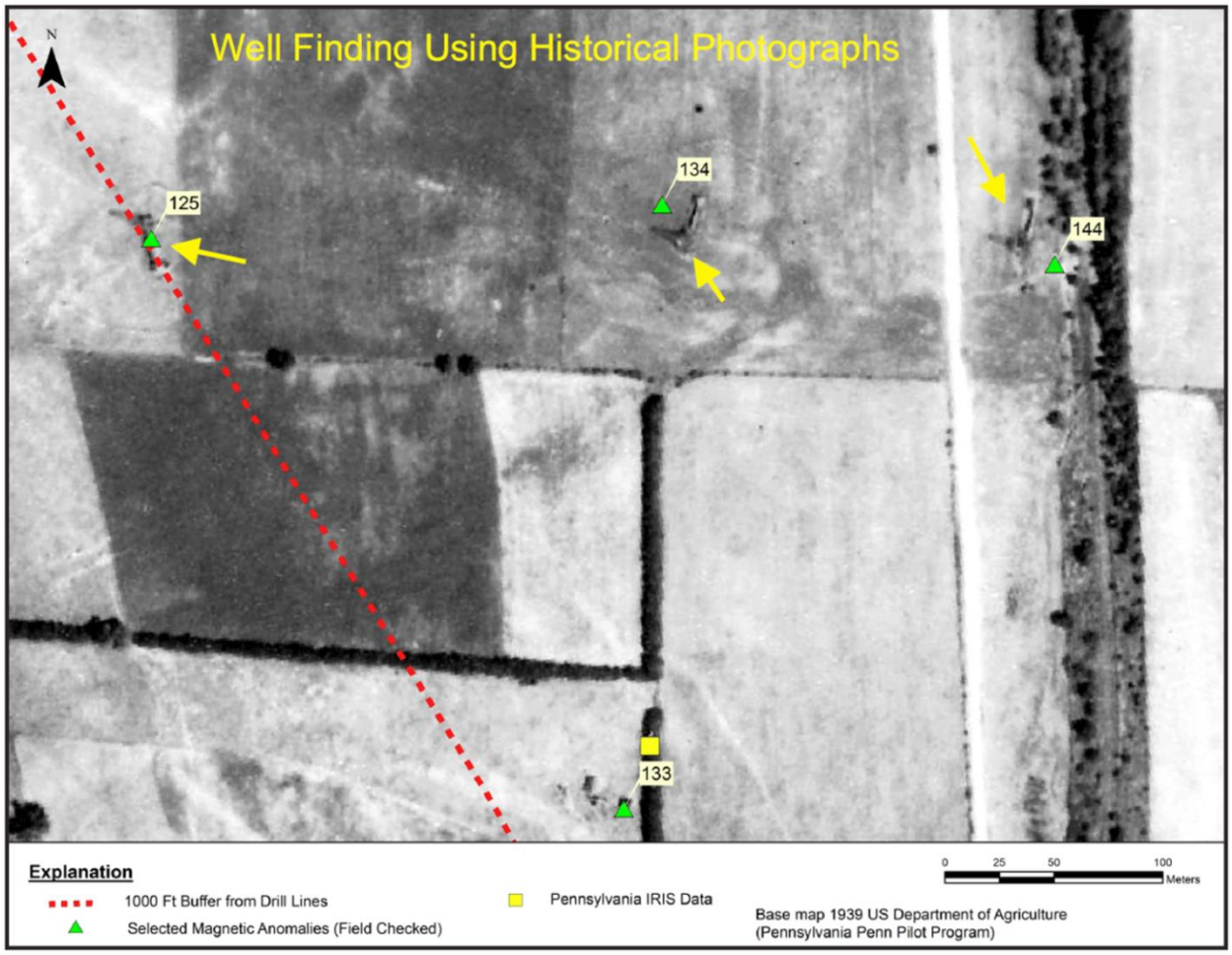

Figure 8: Evidence of well drilling in and around the Study Area, including three well derricks can be seen in this 1939 air photo. The recovered well locations (green triangles) that should be positioned directly below the derricks are instead offset, due to errors from geo-referencing non-orthographic imagery because of inadequate ground control.

2.3 GROUND-BASED INVESTIGATION OF AIRBORNE MAGNETIC TARGETS

A thorough on-the-ground reconnaissance of the magnetic targets was performed from November 2013 to May 2014 on a subset of the original airborne surveyed area. GIS software was used to generate a 1,000 ft. (305 m) buffer surrounding the Marcellus drilling plan originally proposed by the developer (Figure 9). The smaller study area focused the ground search on the buffer area around the proposed horizontal Marcellus wells where state regulators have requested that operators identify existing wells prior to stimulation. NETL's ground reconnaissance consisted of a two or three-person team that focused on confirming that well-type targets identified from airborne surveys were wells. At some well locations, an above-ground well casing was visible, but a portable magnetometer was often needed to locate casing that was either concealed by brush or was cut off below ground.

Navigation to the approximate location of well targets identified during the helicopter magnetic survey was facilitated by the use of a tablet PC running GPS-linked moving maps. However, the ground search was seldom as simple as navigating to the location of the helicopter magnetic anomaly and finding a well. Often, the well was not visible because of the nearly impenetrable undergrowth. Furthermore, GPS receivers were compromised by the thick tree canopy which reduced location certainty. It was also discovered that the selected magnetic targets were assigned to a location along the flight line having the highest TMI. Unless, by chance, the flight line was immediately above the exact location of an anomalous feature, the target location extracted from the aeromagnetic data was invariably offset by several meters.

At several potential well sites where no well casing was observed at the surface, a Geometrics, G-858, portable magnetometer was used to locate the origin of the strongest TMI which was always at the wellhead (Figure 10). The G-858 could be used to collect a continuous stream of magnetic intensity data at a 10 Hz acquisition rate for use in walking surveys. Position data for walking surveys was provided by a backpack-mounted, differentially corrected GPS receiver that would output to the G-858's console data recorder using RS-232 protocol. The G-858 magnetometer's search mode was found to be particularly useful to home-in on strong magnetic sources. Search mode permits the operator to observe the total magnetic field value at the sensor location on a strip-chart display of the unit's data logger console, along with audible pitch changes linked to signal intensity trends in real time. Operating the magnetometer in search mode alone was effective for locating several buried wellheads that were later confirmed by excavation.

Typically, abandoned well sites were littered with a variety of ferro-metallic objects in proximity to the actual well casing location. Many of these objects collectively referred to as oilfield artifacts, included 2-in.-diameter pipe sections or flow lines, steel cable, pulleys, sucker rods, valve assemblies, steel-reinforced concrete footings/pads, dead man anchors, etc. Of particular interest, were hand-forged, square-cut nails that were recovered from several well locations. These nails were commonly used in the late 1800s to early 1900s and served as an unofficial indicator of a wellsite's approximate age. Certain ferro-metallic objects, especially pipes (depending on orientation), can mimic well casing anomalies and may lead to false positives while operating in the magnetometer search mode. The magnetic responses from smaller objects were found to be less of a problem when the magnetic sensor was intentionally held at shoulder height. Unless there was a significant accumulation of these objects and they were more than a few meters from a wellhead, the objects were not resolved as a feature separate from the well casing in the airborne data. The presence of these unresolved objects might explain how some confirmed well anomalies that were expected to appear as symmetrical monopoles also exhibited some dipole characteristics and asymmetry.

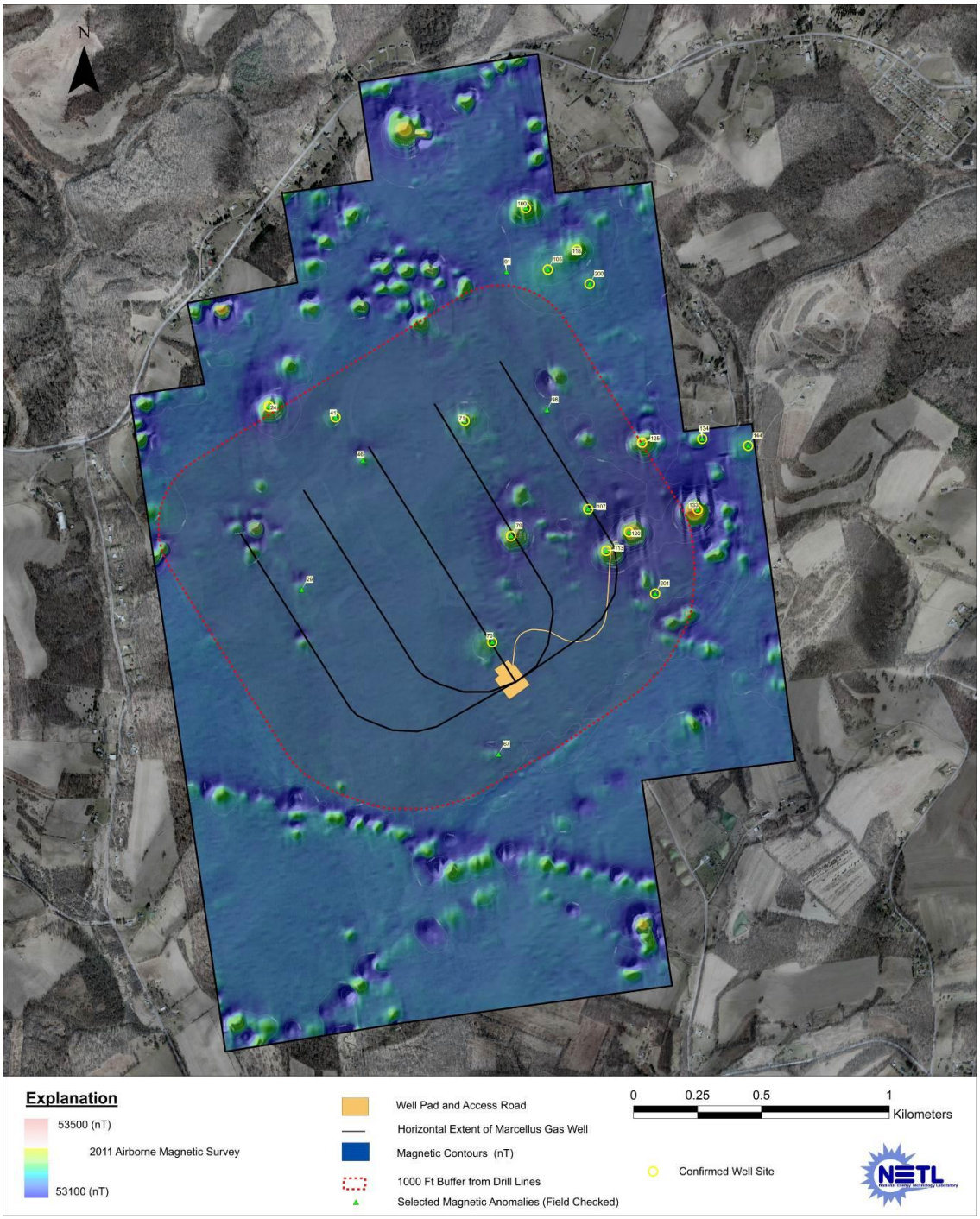

Figure 9: Enhanced TMI aeromagnetic data overlay on a digital ortho, quarter-quadrangle image showing the search area and the locations of wellheads confirmed on the ground.

Walking magnetic line surveys were employed when the identification of an anomalous feature was uncertain. Walking magnetic surveys begin by constructing a regularly spaced grid having multiple line traverses centered on the anomalous magnetic feature from the airborne survey. The walking survey is then performed along each survey line in a serpentine fashion, while the magnetometer sensor is maintained at a constant height above the ground. The magnetometer was operated in simple survey mode, where the magnetic readings are synchronized with GPS locations and stored in the data instrument's data logger. This permits post-processing of the data into color-mapped and contoured grids that may then improve interpretation. Typically, corrections would be made for diurnal fluctuation in the Earth's magnetic field in the magnetic data acquired during a walking survey. However, diurnal fluctuation was usually very small in comparison to the TMI of most well anomalies and therefore, correction was unnecessary under most circumstances. Also, the magnitude of the earth's magnetic field is unlikely to change significantly during the short time interval of most walking surveys (<30 min). Magnetic diurnal correction was used, for instance, at a suspected 1902 wellbore (vide supra), north of the proposed Marcellus pad, where a broad, subtle monopole magnetic anomaly was observed (Figure 10). A base station was not employed, but rather remote data from a magnetic observatory was used to correct for diurnal fluctuations. This approach worked well for the few select open locations where it was employed. Line surveys at most heavily wooded sites were extemporaneous, often following a path of least resistance, or involving a single traverse or traverses intersecting at 90 degrees. Data from this type of survey only required minimal processing, and interpretation was usually simple. The results provide adequate confirmation of monopole, well-type anomalies having a high field gradient, and were deemed acceptable for extracting the true location of the vertical well casings. This approach was necessary in most heavily wooded locations, in combination with search mode and where cutting vegetation or otherwise noticeably disturbing the site would not be permitted by the landowners.

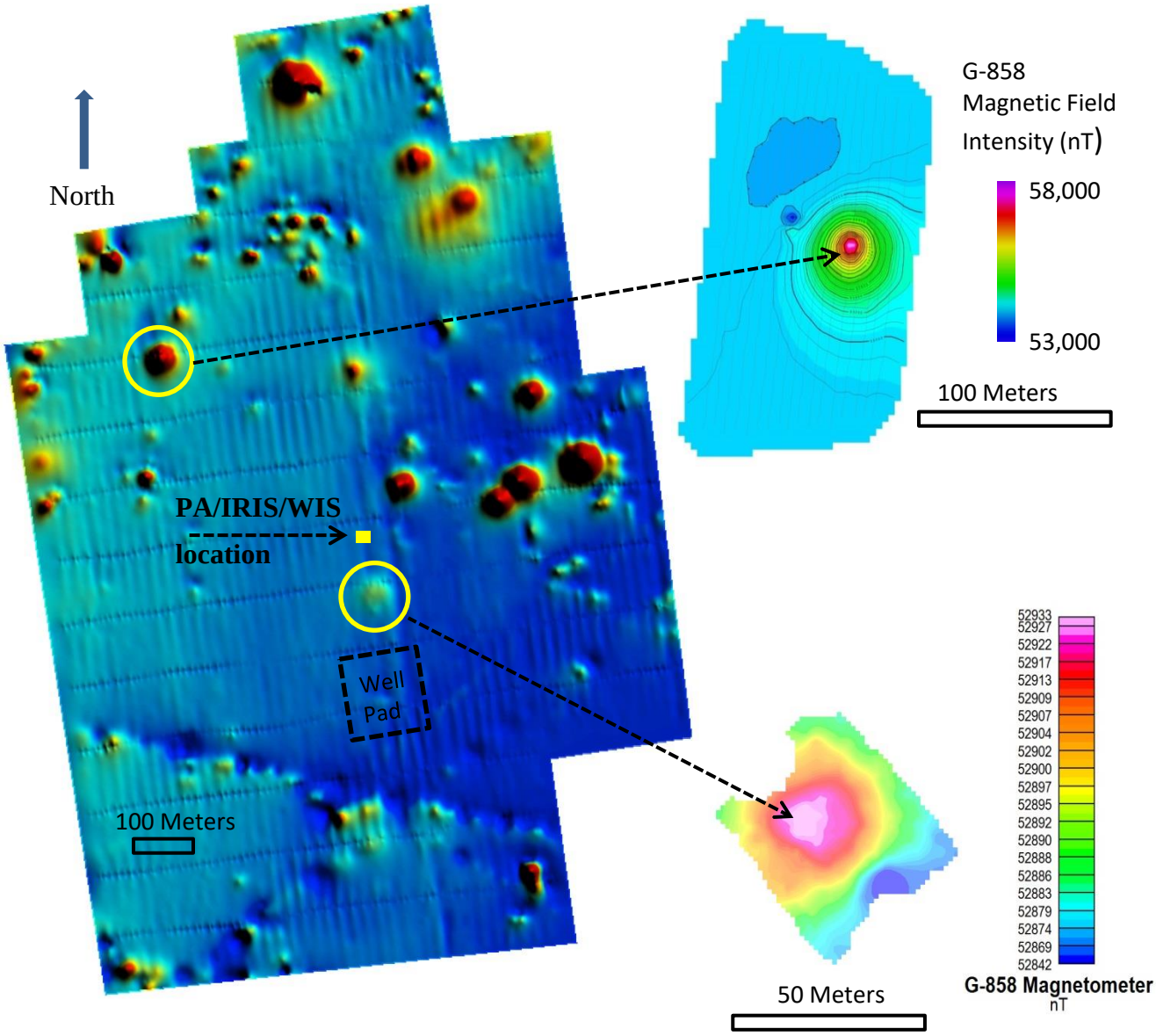

Figure 10: Examples of the gridded results from ground magnetic (walking) surveys conducted over two (circled) suspected wells targeted in the aeromagnetic data. The northernmost unrecorded and unmarked suspected well appears as an intense monopole in the airborne and was confirmed in the ground survey data at right. The broad and subdued monopole anomaly located northwest of the proposed Marcellus well pad is believed to be a known well. The yellow rectangle depicts the Pennsylvania Internet Record Imaging System/Wells Information System (PA/IRIS/WIS) database location for this well.

3. CONCLUSIONS

3.1 AIRBORNE MAGNETIC SURVEYS FOR WELL DETECTION

Aeromagnetic surveys, when properly supported by ground-based validation methods are time and cost-effective methods for locating oil and gas wells. Well-type magnetic anomalies are usually very conspicuous and easily distinguished from other anomalies, having a bull's-eye-like appearance in gridded line surveys and a prominent, nearly symmetrical peak in single traverse surveys. Most, but not all vertical well casings give rise to locally intense induced magnetic fields that are easily distinguished from the magnetic fields arising from ferrous metal objects that are at or near the ground's surface. However, the magnetic detection of wellbores requires there to be at least some steel casing remaining in the wellbore. The magnitude of the magnetic response to well casing is dependent on factors such as: (1) distance from the sensor(s); (2) casing mass (a function of the number of casing strings, casing diameter, and casing length); (3) magnetic susceptibility; and (4) remanent magnetism.

Aeromagnetic surveys for well detection have overcome most of the limitations posed by terrain, vegetation, and access issues and are cost-effective when compared to the number of man-hours that would be required to systematically ground search a large parcel. Historically, ground-based searches for unmarked, abandoned wells have been successful in some areas, but not in areas where dense vegetation limits access and obscures surface evidence of well locations. Thick, brushy undergrowth at the Washington County site concealed many aboveground wellheads, and all but eliminated visual detection of any low cut or buried well casings. The ground investigation found that several abandoned wells sites, easily detected in the aeromagnetic data, showed no visual evidence of the well's location. These wellbores could only be located by conducting ground-based magnetic surveys near the airborne target.

Aeromagnetic survey results can rapidly be screened for the presence of potential wells using software algorithms designed to detect and extract the coordinates for several types of magnetic anomalies. Analysis of the resulting magnetic targets could then be conducted in a GIS. Targets having a high likelihood of being wells were usually spatially related to features in other data layers, such as LiDAR, existing patterns of known wells, or were seen in historic air photos. Six wells at the Washington County site had recorded locations, but these wells would not have been found without the aeromagnetic data because the position error in existing databases often exceeds 100 m (Figure 11). Fifteen of 22 well-type magnetic anomalies targeted for ground investigation using the methods described here were confirmed as abandoned wells. Seven targets were found to be cultural sites unrelated to well development. These included a trash dump, an abandoned truck, a steel-framed trailer, and culvert pipes. Apart from the trash dump, six of the non-well sites presented as magnetic monopoles.

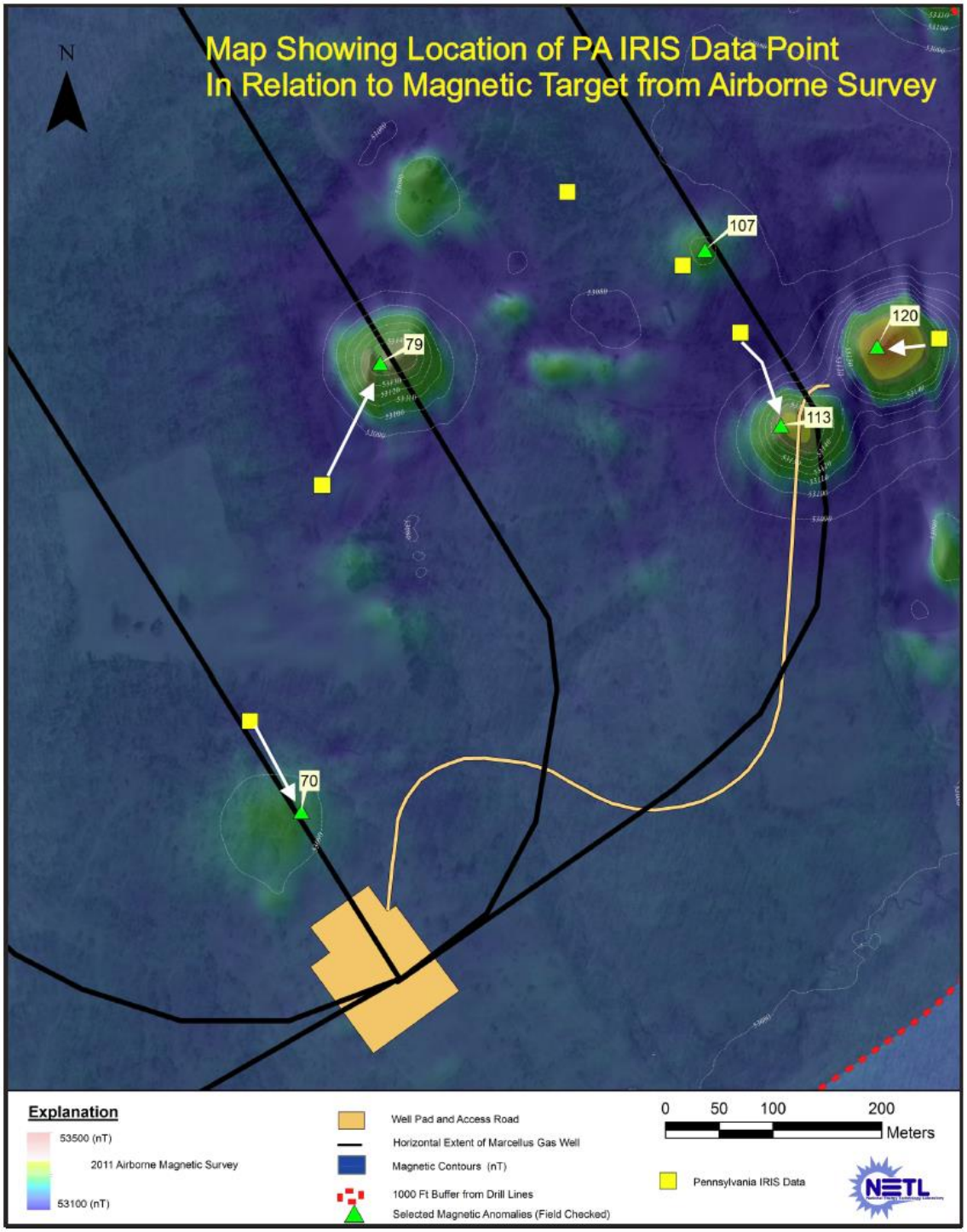

Figure 11: Map showing actual well locations in relation to locations found in the PA/IRIS/WIS database.

3.2 WELL FINDING SUMMARY

The helicopter magnetic survey identified 144 non-pipeline-related magnetic targets within the flight area. Of these, 123 targets are believed to be steel-cased wells based on their monopolar magnetic anomalies—either oil and gas wells or wells for residential water supply. Within the Pennsylvania Department of Environmental Protection (PADEP) recommended 1,000-ft-wide buffer area surrounding five proposed horizontal Marcellus Shale wells, 22 well-type magnetic targets were identified based on the initial inspection of the helicopter magnetic data. A ground reconnaissance found that 15 of 22 well-type magnetic targets were wells; and 7 magnetic targets were from non-well sources including trash dumps. Further investigation using a combination of airborne magnetic data, LiDAR (topographic footprint-showing a pad or access road), and historic 1930s aerial photography (showing derricks and pump houses) identified three additional well locations for a total of 18 well locations within the PADEP buffer area. The ground investigation confirmed all 18 historic well sites: two wells are still in production and are included in the six sites that are listed in the PA/IRIS/WIS database. The remaining 12 wells were unmarked, abandoned, and undocumented.

The ground investigation found that well locations from the PA/IRIS/WIS database were often more than 50 m from the actual well location; this large error could contribute to difficult and often unsuccessful ground searches when wells are concealed beneath heavy vegetation. The well targets from the aeromagnetic survey were more accurate, being within 5 m of the actual well location. Yet a portable magnetometer was still needed at 6 of 18 sites to locate the well casing in heavy brush cover. A LiDAR topographic well footprint was visible at 7 of 18 well locations. At 6 of 18 well locations, derricks and pump houses could be seen on historic geo-referenced photographs.

This study demonstrated the ability of helicopter magnetic surveys to detect a well where near-surface casing had been removed leaving only deeper casing in place. The broad and subtle monopole target observed in the aeromagnetic survey (Figure 11, magnetic target # 70) is believed to be the location of a well where handwritten records state that the operator removed the upper casing but the deeper casing became stuck and was left in the hole. Modeling of results from ground magnetometry and DC resistivity methods indicate that the depth to the top of the remaining casing is approximately 60 ft (Appendix A). Despite being buried 60-ft below ground, the magnetic anomaly from the remaining well casing was detected by the helicopter magnetic survey.

Table 1 is a synopsis of evidence used to locate 18 abandoned wells within the PADEP 1,000-ft-wide buffer area surrounding five proposed horizontal Marcellus Shale gas wells.

Table 1: Number of Confirmed Well Sites and Non-Well Sites Located within the Study Area Using Well Location Tools Described in this Report

Sites	PA/IRIS/WIS	Aeromagnetic	1930s Imagery	LiDAR	Ground Magnetics	Total Sites
Wells	6	15	6	7	6	18
Non-wells		7				7

3.2.1 Effects of Aeromagnetic Survey Flight Line Spacing on Well Identification

The airborne magnetic survey method, as employed in this study, is too expensive for abandoned well location in smaller areas, such as the PADEP buffer areas around well pads with multiple horizontal wells. NETL's design for the current survey was based on lessons learned from previous aeromagnetic surveys conducted for locating unmarked wells in early oilfields, where a high density of wells was sometimes common. The ability to resolve closely spaced wells is a challenge for airborne magnetic methods; the simplest mitigation is to either reduce the distance between flight lines or fly closer to the ground. Closer flight line spacing was favored because of safety concerns about low-altitude flight.

The nominal line spacing used at the Washington County site was 25 m. Even with 25-m flight line spacing, some known wells less than 15-m apart were not resolved as two distinct magnetic anomalies (Veloski, 2008). This was especially true whenever adjacent wells differed greatly in magnetic response or when the prescribed survey altitude over the closely spaced features was significantly exceeded. The helicopter was configured with two sensors mounted approximately 12 m apart. Therefore, the effective line spacing was much closer when the data from each sensor were treated separately. Processing the data separately has been found to improve the resolution of closely spaced magnetic features (Hammack et al., 2006).

Because increasing flight line spacing for the aeromagnetic survey reduces cost, an exercise was performed to determine the maximum flight line spacing that could be used without overlooking any of the 15 confirmed well targets in this study. Interline spacing was synthetically increased by manually deselecting flight lines from the Geosoft line database and reprocessing. Nominal spacings of 50, 75, and 100 m were then compared to the original 25 m dataset. Figure 12 shows gridded images generated by sequentially reducing the flight line density in this fashion and re-gridding to determine which interline spacings would still allow visual detection of the same wells confirmed in the field. The gridding method was minimum curvature and cell size was 25% of the nominal line spacing, an accepted practice (Sequent, 2023). Based on the results from this test, it may be concluded that a flight line spacing of 50 m could have been used without missing any confirmed wells. Only widely separated, high TMI wells could be identified in the imagery processed with synthetic 75- and 100-m flight line spacing.

The cost of aeromagnetic surveys can be reduced by: (1) flying larger area to receive a discount line-kilometer rate or (2) consolidating multiple, geographically close areas to eliminate mobilization fees and associated costs incurred with multiple deployments of the flight crew and technicians.

Table 2: Effect of Flight Line Spacing on the Detection of Confirmed Well Anomalies

	25 m	50 m	75 m	100 m
Confirmed well anomalies observed in aeromagnetic grids	15	15	10	8

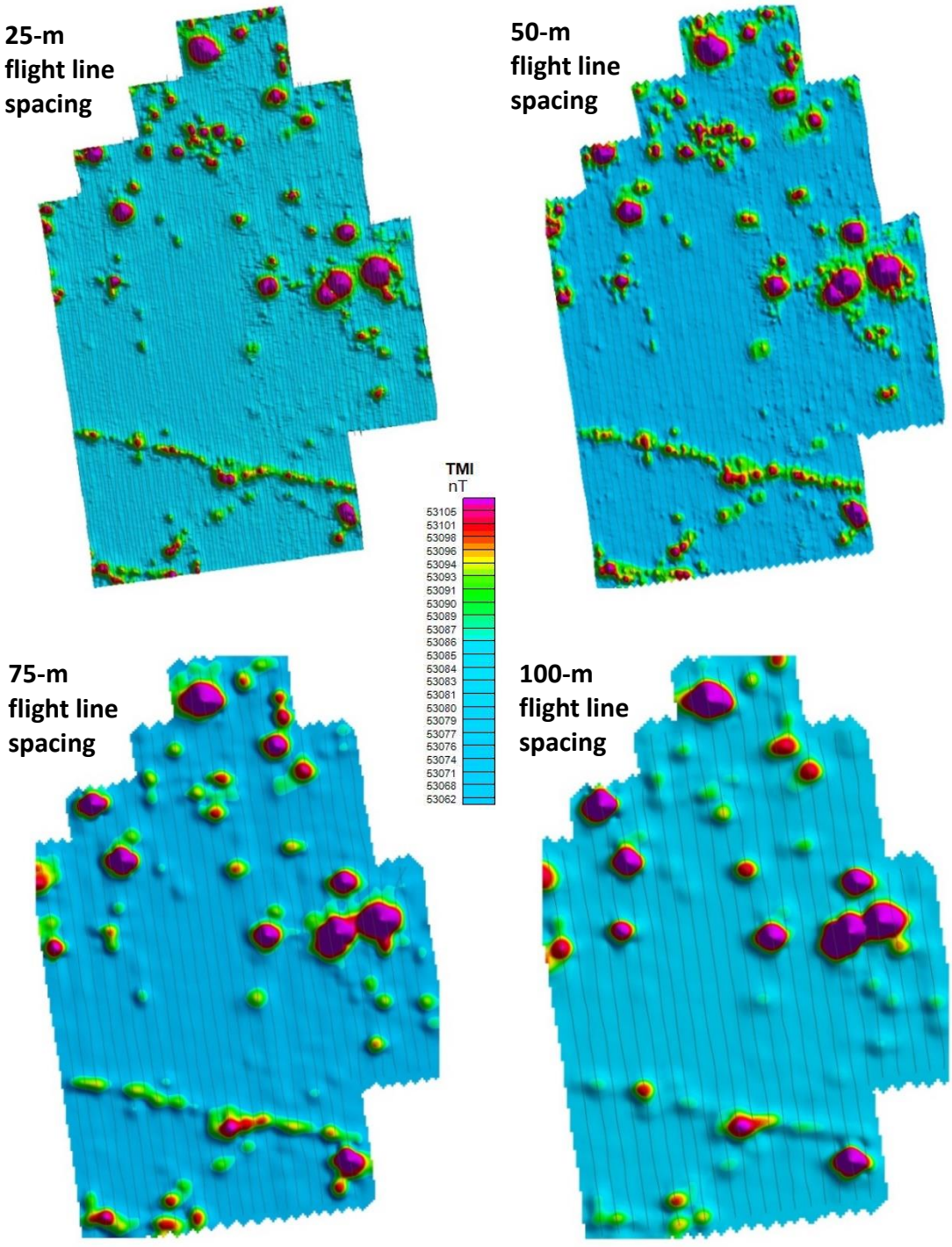

Figure 12: Minimum curvature grids generated from analytic signal processed aeromagnetic data at the Washington County site. The line intervals from the original dataset were synthetically reduced and the resulting data re-gridded at the appropriate cell size.

This page intentionally left blank.

4. REFERENCES

Airports Guides. Climate and weather guide; Pittsburgh International Airport. http://www.pittsburgh-pit.airports-guides.com/pit_climate.html (accessed on December 9, 2021).

Armstrong, F. E. *Locating uncharted oil and gas wells: state-of-the-art*; TPR 65; U.S. Bureau of Mines, 1973.

Baer, L. J.; Overfelt, R.; Faile, T. Total field magnetic surveys to locate abandoned wells: three case histories. *The Leading Edge* **1995,** *14*, 237–241.

Barret, W. M. *Magnet Disturbances caused by buried casing*; Bulletin of the American Association of Petroleum Geologists: Tulsa, OK, 1931; pp. 89–105.

Barrows, L.; Rocchio, J. E. *Magnetic Surveying for Buried Metallic Objects*; Ground Water Monitoring Review, 1990.

Bowman, I. *Well-drilling methods*; USGS Water Supply, 1911.

Breiner, S. *Application Manual for Portable Magnetometers*; Geometrics, Inc.: San Jose, CA, 1973; pp. 58.

Commonwealth of Pennsylvania, Pennsylvania Statutes Title 58. Oil and Gas Section 601.203 - Well registration and identification (accessed on Nov. 1, 2024).

Dilmore, R. M.; Sams, J. I.; Glosser, D.; Carter, K. M.; Bain, D. Spatial and Temporal Characteristics of Historical Oil and Gas Wells in Pennsylvania: Implications for New Shale Gas Resources. *Environmental Science & Technology* **2015,** *49*, 12015–12023. DOI: 10.1021/acs.est.5b00820.

Friedman, S. J.; Stamp, V. *Teapot Dome: Site Characterization of a CO_2-Enhanced Oil Recovery Site in Eastern Wyoming*; UCRL-JRNL-217774; Lawrence Livermore National Laboratory, 2005.

Frischknecht, F. C.; Grette, R.; Raab, P. V.; Meredith, J. *Location of abandoned wells by magnetic surveys; acquisition and interpretation of aeromagnetic data for five test areas*; USGS Open-File Report 85-614A; 1985.

Hammack, R. W.; Veloski, G. A.; Hodges, G. Helicopter Magnetic Surveys for locating wells and oilfield infrastructure. Paper presented at the International Petroleum Environmental Conference (IPEC), San Antonio, TX, Oct 17–20, 2006.

Herman, R. An Introduction to Electrical Resistivity in Geophysics. *Am. J. Phys.* **2001,** *69*. (accessed Mar. 31, 2014).

Land, L.; Veni, G. *Electrical Resistivity Survey: I&W Brine Well, Eddy County, New Mexico*; National Cave and Karst Research Institute Report of Investigation 2, Carlsbad, NM, 2011. nckri-report-of-investigations-02.pdf (accessed on Aug. 22, 2024).

Luyendyk, A. P. J. Processing of Airborne Magnetic Data. *J. of Australian Geology & Geophysics* **1997,** *17*, 31–38.

Martinek, B. C. Ground Based Magnetometer Survey of Abandoned Wells at the Rocky Mountain Arsenal-A Case History. Symposium on the Application of Geophysics to

Engineering and Environmental Problems, 1988; pp. 578–596. https://doi.org/10.4133/1.2921812

PA Oil and Gas Mapping. PA Oil and Gas Mapping (accessed on Aug. 22, 2024).

Pennsylvania Spatial Data Access Website. Pennsylvania Spatial Data Access (psu.edu) (accessed on Dec. 16, 2021).

Sams, J. I.; Edenborn, H. M.; Fagley, P. J. Using LIDAR to Locate Historic Drilling and Charcoal Production Sites in Pennsylvania. Geological Society of America Annual Meeting, Charlotte, NC, Nov 4–7, 2012.

Sevon, W. D., compiler. Physiographic provinces of Pennsylvania (4th ed.): Pennsylvania Geological Survey, 4th ser., Map 13, scale 1:2,000,000, 2000. (accessed on Aug. 22, 2024).

Sequent.https://help.seequent.com/Oasismontaj/2023.2/Content/gxhelp/c/geosoft_gx_channelstogrid.htm (accessed on Aug. 20, 2024).

Sheriff, R. A. First Course in Geophysical Exploration and Interpretation; 1978.

Veloski, G. A.; Hammack, R. W.; Stamp, V. W.; Colina, K. Helicopter Magnetic Survey at the Teapot Dome Oilfield (Naval Petroleum Reserve NO. 3) - A Case History. Paper presented at the Symposium on the Application of Geophysics to Engineering and Environmental Problems (SAGEEP) 2008 Annual Meeting of EEGS, Philadelphia, PA, 2008.

Xia, J.; Williams, S. L. High-resolution magnetic survey in locating abandoned brine wells in Huchinson, Kansas. Paper presented at the Symposium on the Application of Geophysics to Engineering and Environmental Problems (SAGEEP) 2003 Annual Meeting of EEGS, Las Vegas, NV, April 6–10, 2003.

APPENDIX A: ESTIMATING DEPTH TO WELL CASING

At some well locations, the near surface casing has been removed, but casing remains at depth. To re-enter these wells either for repurposing or for plugging, it is helpful to know the depth to casing. Figure A1 contains a broad, low intensity monopole (well-type) magnetic target that is of particular interest because it is located within 200 m of a proposed Marcellus Shale drill pad. The anomaly appears approximately 100 m northwest of recorded well 125-90300 appearing in the PA Oil and Gas Mapping website (PA Oil and Gas Mapping). Well 125-90300 was drilled in 1902, and described as a dry hole with a total depth (TD) of 2,510 ft. The TD suggests the target formation is the Venango Sand based on records from wells drilled to a similar depth in the area. The well record also indicates that the casing had been pulled, and a section of 10-in. diameter casing was described as "lost in hole" at some unspecified depth belowground. The length of casing remaining in the well is uncertain because a hole punch cored away the numeral immediately preceding a zero (0) on the hand-written paper record. This implies that the lost section of casing would be ≥10 ft in length. The broad, low intensity magnetic anomaly probably arises from the lost section of 10-in. pipe because the lower-than-expected magnetic intensity is consistent with well casing buried some unknown distance belowground (further from the helicopter magnetic sensors). Magnetic falloff with distance can be used to distinguish between dipole and monopole anomalies and to estimate the depth of the feature below surface using a processing technique known as continuation.

Ground reconnaissance efforts were focused on locating well 125-90300 because of its proximity to the proposed Marcellus Shale drill pad and because it is suspected to be an open wellbore. A differentially corrected GPS receiver was used to navigate to the coordinates of the magnetic target identified by the helicopter survey. The location showed evidence of disturbance in the LiDAR topographic imagery, but no conclusive surface evidence of a well was found. A Geometrics G-858, GPS-linked, cesium-ion magnetometer was used to conduct a survey consisting of seven parallel lines having 10-m interline spacing in a 60-m x 100-m area centered on the airborne magnetic target. The magnetic data were diurnally corrected, gridded with 2 m cell spacing, and presented in Figure A1 with an overlay of the aeromagnetic field contours. The centroid of the apparent monopole anomaly from the ground magnetic survey coincides with the centroid of the magnetic anomaly from the helicopter survey. A few minor magnetic anomalies were also noted in the profile data from the ground survey, likely originating from ferrous metal artifacts at the surface near the probable wellbore.

Additional geophysical investigations at the well 125-90300 location were undertaken to determine the depth to the top of the casing lost down-hole. Knowing this depth is important because the downhole casing was detected by the helicopter magnetic survey. Anecdotal evidence suggests that there might be many abandoned wells like this one where some casing was pulled for salvage or reuse. The detection of these open wellbores is a priority because of the threat that they can pose to drinking water aquifers and surface structures. Knowing the amount and depth of casing needed for detection by helicopter magnetic surveys is helpful for predicting the utility of this method for locating wells with partially pulled casing. From a modeling perspective, it is important to understand the relationship between the magnetic signal intensity and the remaining mass of well casing and its depth. This could help determine the practicality of using this method to detect wells where casing remains at some depth underground.

There are a few commonly accepted methods for estimating depth to magnetic source that are based on signal intensity and are directly applicable to the magnetic data. These include

maximum slope method, Peters (half-slope) method, nomograms, Euler deconvolution, and the Werner deconvolution. The simplest of these methods involves calculating half-widths and straight-line slope distances of individual peak profiles. This type of simple modeling is only applicable to spherical dipoles or monopoles arising from vertically oriented cylinders and therefore should provide good depth estimates for well-type anomalies. The half-width method depends on the measurement of the width of the peak along its baseline between the location of maximum intensity and half maximum intensity. The half-width distance is then multiplied by the factor 1.3 to estimate the depth to the top of the monopole anomaly (Breiner, 1973). The slope method requires finding the best straight-line fit along the flank of a symmetrical peak and measuring the distance along the x-axis where vertical lines drawn from the best-fit endpoints intersect the x-axis. This distance is then multiplied by an empirically derived factor $0.5<k<1.5$. Since the magnetic data was acquired from aloft, the absolute altitude of the helicopter (obtained from the laser altimeter data channel) must then be subtracted from this intermediate result.

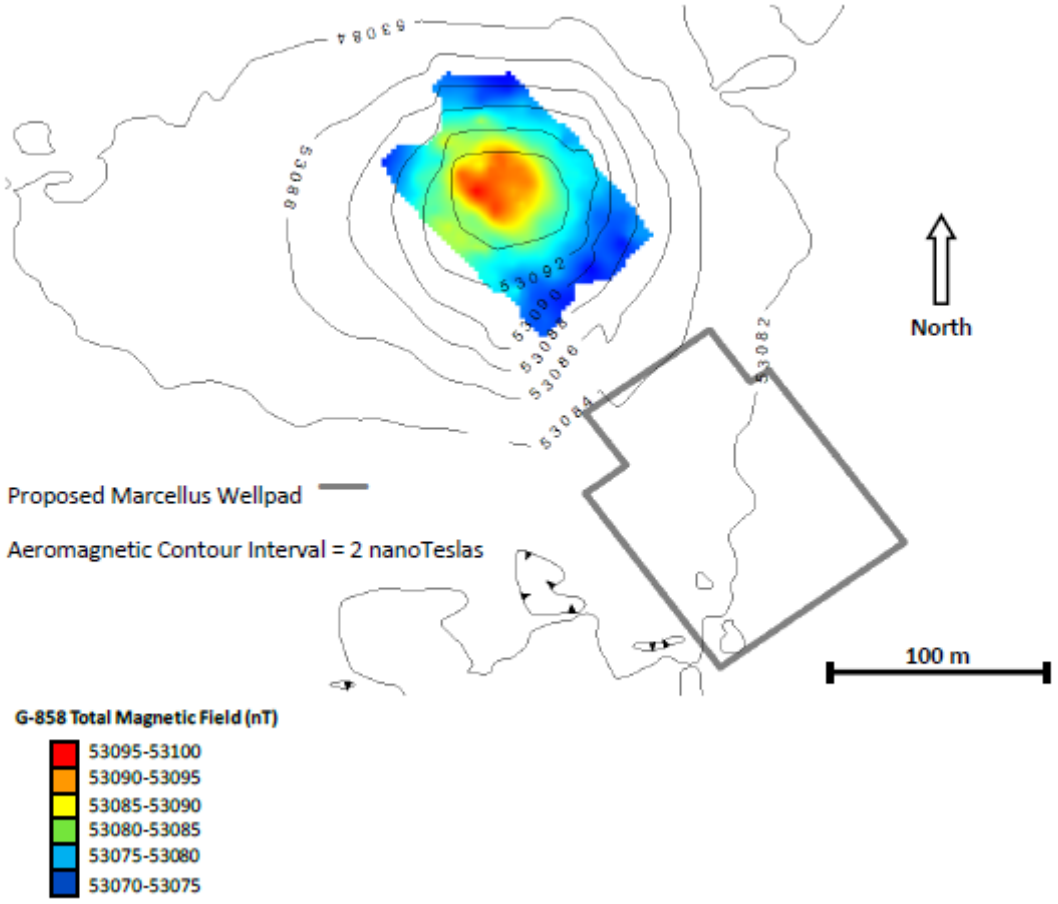

Figure A1: Overlay of aeromagnetic total field contours on color mapped, G-858 ground-based magnetic survey of an anomaly near known well 125-90300.

The horizontal gradient method (Peter's slope method) is based on first calculating the slope of the anomaly from the best linear fit (as determined by the correlation coefficient) at the point of inflection, tangent to one side of a symmetrical peak. The half-slope is then calculated and the distance between these two points on the magnetic profile that are parallel and tangent to the half-slope line determine the approximate depth to the top of the magnetic body (Sheriff, 1978). The method also relies on "index values" that range from 1.2 to 2.0 that compensate for variations in magnetic moment. The accuracy of these methods has been reported as "fair to good" for magnetic inclinations of 90°. The magnetic inclination of the Washington County study site was approximately 68°. If the data are acquired along close parallel swaths, a strong magnetic anomaly may be observed on several adjacent lines. Under these circumstances, the line containing the anomaly having the highest maximum intensity would be selected to improve the signal to noise relationship. The anomaly representing the suspected well was observed on five adjacent flight lines that include a perpendicular-oriented tie-line.

To evaluate the accuracy of the half-width and straight-line slope distance methods, airborne magnetic data were extracted along a peak profile arising from overflight of a confirmed vertical well casing that emerged 1 m above the ground (Figure A2). Both calculations provided nearly identical approximations, by estimating the depth to be nearly level with the ground at the location of the anomaly.

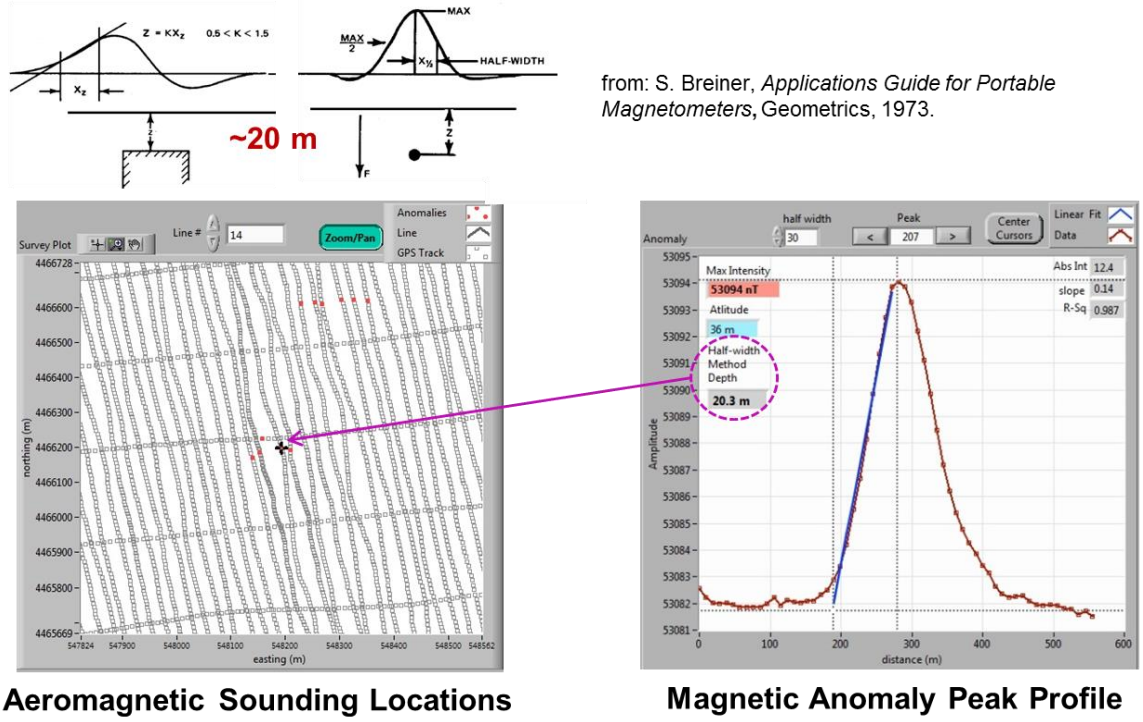

Figure A2: A subset of the aeromagnetic line profile data centered over suspected well 125-90300. The peak profile was used to estimate depth to the top of the magnetic feature (lost casing) employing both half-width and slope methods. The peak profile in the right panel was constructed from 60 consecutive magnetic soundings centered over the black cursor location along the flight line depicted in the panel on the left. The red dots indicate other sounding locations representing the center of the same anomaly (peak) that appears on multiple adjacent flight lines.

The National Energy Technology Laboratory (NETL) also used earth resistivity (ER) data collected on the ground above the wellbore in an attempt to determine the depth to the lost section of well casing. The ER method offers the ability to measure the two-dimensional (2D) distribution of subsurface resistivities and to estimate depth to geologic features through a numerical analysis of these measurements made along an array of regularly spaced electrodes that are driven into the ground (Figures A3, A4, and A5). The experimental design employed 56 electrodes spaced 2 m apart for a total of 110 m. The electrode array was deployed along a line centered on the location of the highest measured magnetic intensity from both the airborne and ground-based surveys (Figure A6). The depth of exploration of the method is limited by the length of the array and attenuation of injected current due to the resistance through the measurement path. The depth is also dependent on the array interrogation geometry used.

NETL utilized an AGI SuperSting R8 instrument to acquire resistivity data at the study site. The SuperSting R8 applies current at low frequency between one pair of electrodes and simultaneously measures the resulting potential between multiple electrode pairs at predetermined positions along the array. The sequencing and location of the current/potential electrode pairs are unique to the geometry of the resistivity imaging experiment. This instrument is equipped with multi-conductor cables capable of addressing electrodes and switching operations from current injection to potential measurements in a distributive fashion as the scan progresses. The pattern of interrogation of the electrodes is automated by a control unit and handled programmatically under the instruction of a sequential commands file. Dipole–dipole and Wenner Array geometries were employed in the surveys to emphasize both near-surface features and those at depth. Additional statistical processing was also applied to remove noisy data prior to inverting.

Resistivity, ρ, is a constant of proportionality derived from the measurement of resistance (R) along the length of a uniform cylinder and is a physical property of a pure material:

$$R = \rho(L/A) \qquad \text{where L= length and A= area} \qquad \text{(A1)}$$

The total resistance can then be determined by measuring the potential difference throughout a cylinder where a known current is applied in accordance with Ohm's Law:

$$R = V/I \qquad \text{where V=potential difference and I=transmitted current} \qquad \text{(A2)}$$

One conceptual model for the Earth can be thought of as consisting of a homogeneous and isotropic half-space medium. In this case the potential at any point in that medium may be determined by:

$$V = \rho I/2\pi r$$

Where:

V=potential difference (volts),

ρ is the resistivity of the medium,

I is current in amperes,

and r is the distance to the electrode.

Apparent resistivity (ρ) then by substitution and rearrangement,

$$\rho=(V/I)(A/L)=RA\ K \quad \text{(A3)}$$

Where RA, is the apparent resistance and, K, is referred to as the geometric factor which describes the geometry of the hypothetical cylinder through which the current flows. The geometric factor term K involves the specific geometrical distribution of measurements and are important experimental parameters that have evolved with the technique. Depending on the type of electrode configuration and pattern of current injection and potential measurements, can enhance subsurface geoelectrical features in the horizontal or vertical direction. Equation A4 shows the geometric factor (K) for a dipole-dipole array.

$$\pi\alpha n(n+1)(n+2) \quad \text{(A4)}$$

Apparent resistivity (ρa) is then calculated from the ratio of current to measured potential according to Equation A5.

$$\rho a=\pi\alpha n(n+1)(n+2)(V/I) \quad \text{(A5)}$$

ER data collected at the Washington County site utilized both dipole-dipole and Wenner arrays. The dipole-dipole array current injection dipole (A, B) and potential measurement dipoles (M, N) are closely spaced and equidistant. Dipole-dipole arrays are useful for the measurement of lateral changes in resistivity. Wenner array data are more quickly acquired and show a better response to shallower features. Figure A3 shows the geometry for the dipole-dipole electrode configuration that was used primarily to explore the abandoned wellbore.

One conceptual model for the Earth can be thought of as consisting of uniform horizontal layers. Since the resistivity of various layers can differ by several orders of magnitude, homogeneous geologic layers can be classified according to their corresponding resistivities. An example would be more conductive materials such as clays (1–20 Ωm) are easily distinguished from a layer of limestone (103–106 Ωm).

The inversion results from the ER survey over the well 125-90300 site showed some notable features. To reduce uncertainty in the inversion results, particularly at depth, the dipole-dipole and Wenner survey data were merged (Figure A6). Merging these datasets not only increases data density but has the added benefit of increasing resolution of details at the shallower depths. Additional statistical processing was performed in Earth Imager™ to eliminate excessively noisy input data from the inversion. The resulting resistivity cross-section showed a prominent, vertically oriented feature of low resistivity (5 ohm-m) approximately 20 m below the surface, extending downward to the depth of exploration (26 m). The feature was centered on the position of highest magnetic intensity and at the location of the suspected well. There was a more resistive layer 10 m thick above the suspected wellbore extending the length of the survey line. This probably consists of more resistive bedrock that was also evident in a GEM-2 inductive electromagnetic survey conducted over the nearby Marcellus Shale gas well pad. The surface down to approximately 4 m shows a conductive zone—possibly a clay layer extending to the surface in several locations. Shallow clay was found while exploratory digging in the area. Water saturated soils can also reduce apparent resistivity. The exact depth to groundwater at this location was not determined.

A reasonable hypothesis is that a steel casing would provide a less resistive or short circuit path through which current flow would be channeled during an ER experiment, provided it was between the electrode pairs and relatively close to the surface. There is the strong supporting evidence of a vertically oriented ferromagnetic object over which the ER electrode array was intentionally centered. Even if the casing had partially rusted away, a subdued magnetic anomaly would persist and at least some increase in conductivity would also be expected due to-products from corrosion acting as electrolytes in the surrounding soils where the casing had been. The uncertainties remaining are whether the casing can be observed within the depth of exploration of the ER array and if so, how a vertically oriented conductive body manifests itself in an inversion image. Fortunately, these hypotheses are supported by at least one similar example in the literature, although none could be found that replicate the exact circumstances in this experiment. A resistivity survey used to find evidence of brine-filled cavities from solution mining in New Mexico (Land and Veni, 2011) showed a conductive feature in the inversion results when an ER survey line was within 2 m of an open, abandoned brine well. The report was not clear whether steel casing was actually observed. A somewhat lower resistivity on the order of 1 ohm-m was observed in that study and was concluded by the authors to be indicative of a brine filled cavity. Had steel casing been present, a similar result would be expected.

The information recorded in the PA/IRIS/WIS indicated that suspected well 125-90300 at the Washington County site had a recorded depth of 2,510 ft and that the Venango Formation was the target. Nearby wells of comparable total depth (1,938–2,510 ft) reported production from the Venango. The water in the Venango formation is suspected to be brine and would therefore be highly conductive. The well was also described to be a dry hole, and the casing was salvaged for reuse. Plugging of wells was not customary and prior to 1921, not a legal requirement. An unplugged wellbore could serve as a lower resistance vertical pathway for the movement of fluids. This may even be possible if an uncased wellbore had collapsed because the former borehole would be filled with less consolidated material and could be hydraulically connected with groundwater closer to the surface. If the top of the vertically oriented, narrow conductive pod as seen in the inversion results (Figure A6) represents the bottom of the vadose zone, a localized increase in salinity near the wellbore column could be another possible explanation for the conductive feature observed in the ER inversion image. The ER inversion model yielded an estimated depth to the lost casing section of approximately 20 m. This distance was determined directly from the inversion profile image (Figure A6). This processing result was accomplished using the default (recommended) input parameters in Earth Imager™ and in combination with statistical preprocessing to remove noisy data. It should be noted that by changing the model input parameters the estimated depth could be made to vary. It was also possible to eliminate the anomaly entirely by further altering these parameters. Therefore, results derived from these types of modeling experiments should be approached cautiously.

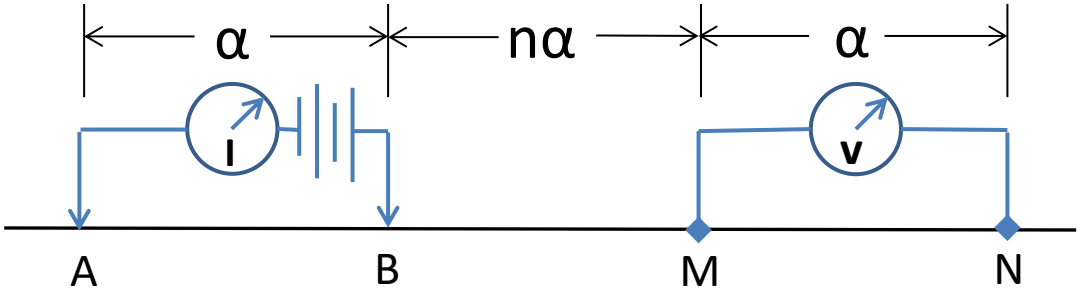

Figure A3: Dipole-dipole electrode configuration. The dipole electrodes are spaced equidistant while the spacing between electrode pairs is an integer multiple of the electrode spacing. The distance between dipole centers is restricted to α(n+1). 2π (1/r_Am -1/r_Bm - 1/r_An +1/r_Bn) is the geometric factor (K) used for calculating apparent resistivity for the dipole-dipole data array. Where rAm and rBm are the distances from potential electrode m to current electrode A and B, and rBm and rBn are distances from potential electrode n to current electrode A and B.

Figure A4: NETL Researcher operating a resistivity instrument over a suspected abandoned well appearing in the PA/IRIS/WIS database. The record for this 1902 well describes it as a dry hole having a section of casing lost at an unknown depth during a salvage-for-reuse operation. These data were inversion-modeled to estimate the depth to the top of the well casing.

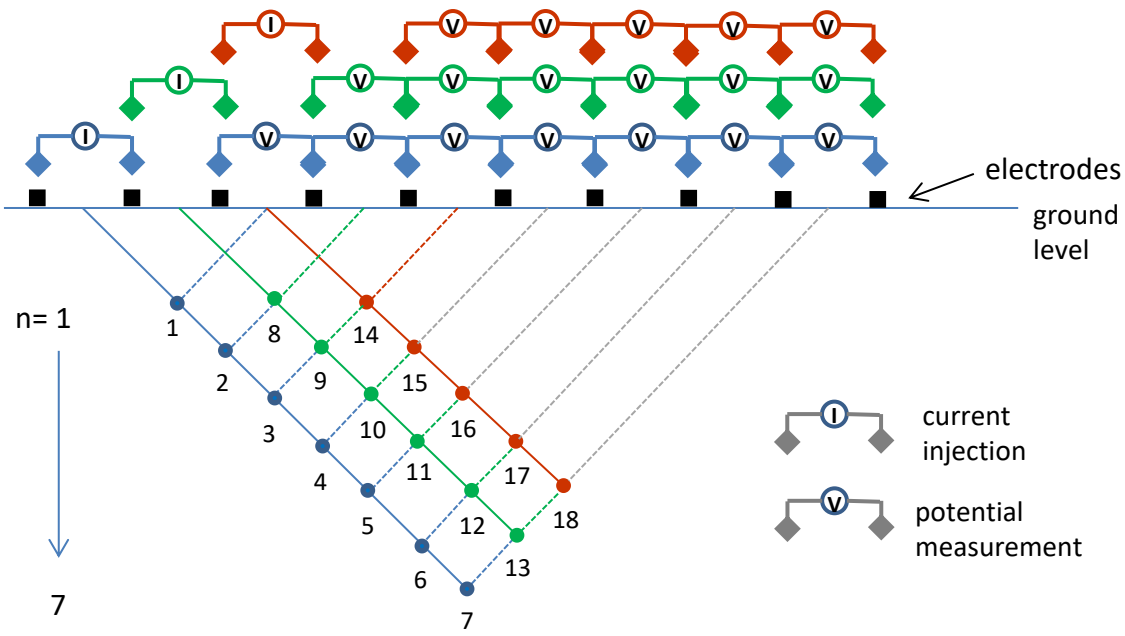

Figure A5: Continuous resistivity survey profile schematic showing three iterations of dipole-dipole geometry data acquisition sequencing.

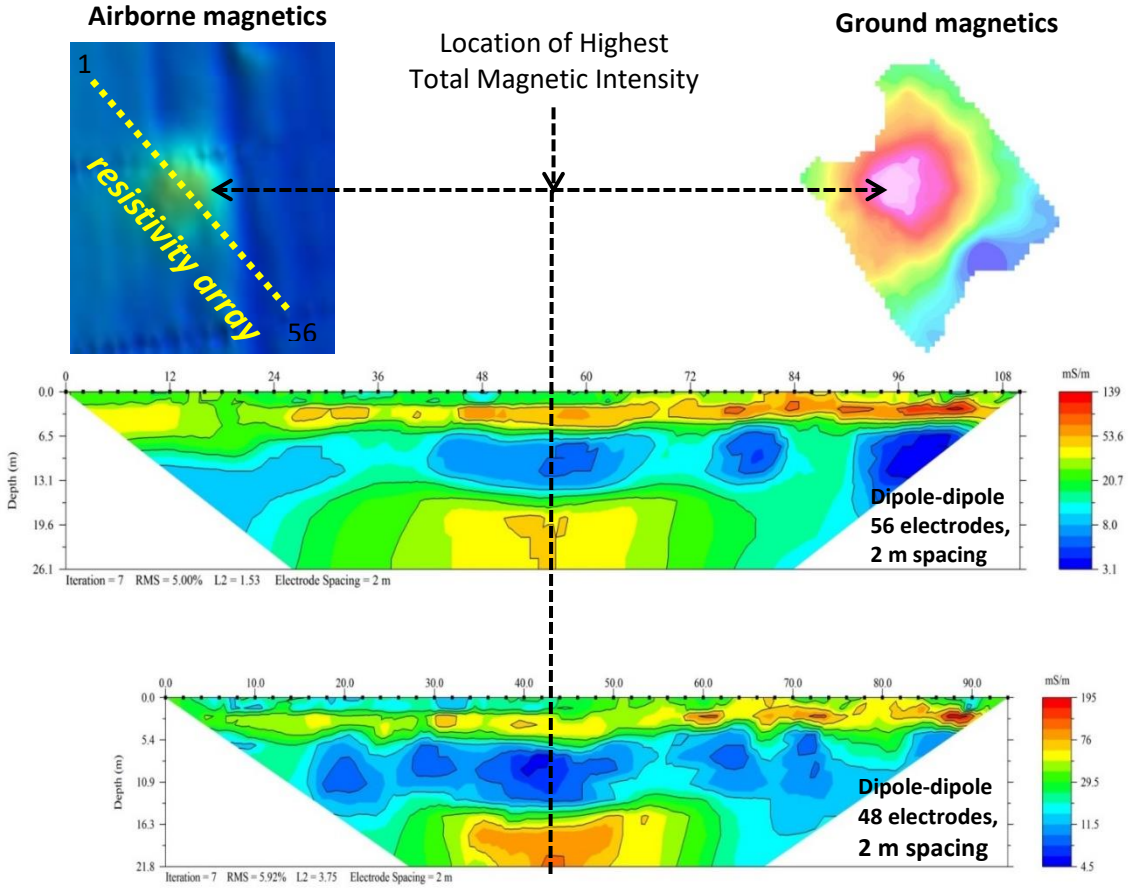

Figure A6: Resistivity survey results showing merged dipole-dipole/Wenner array inversion (top) and dipole-dipole array inversion (bottom). The conductive anomaly at depth in both images is believed to be generated by the lost section of casing. The lower image shows the same anomaly offset 14 m corresponding precisely to the removal of the first eight electrodes from the left of the array.

This page intentionally left blank.

APPENDIX B: FUGRO AIRBORNE MAGNETIC SURVEY REPORT 12024

This page intentionally left blank.

Marianne Walck
Director
National Energy Technology Laboratory
U.S. Department of Energy

Bill Fincham
Technology Manager
Methane Mitigation Technologies
National Energy Technology Laboratory
U.S. Department of Energy

Andrew Govert
Program Manager
Undocumented Orphan Well Program
Office of Fossil Energy and Carbon Management
U.S. Department of Energy

Natalie Pekney
Technical Portfolio Lead
Undocumented Orphan Well Program
National Energy Technology Laboratory
U.S. Department of Energy

NETL Technical Report Series